

1
2
3
4
5
6
7
8
9
10
11
12
13
14
15
16
17
18
19
20
21
22
23
24
25
26
27
28
29
30
31

6mer seed toxicity in tumor suppressive microRNAs

Quan Q. Gao^{1,6}, William E. Putzbach^{1,6}, Andrea E. Murmann¹, Siquan Chen², Aishe A. Sarshad³,
Johannes M. Peter⁴, Elizabeth T. Bartom⁵, Markus Hafner³, and Marcus E. Peter^{1,5,*}

¹Department of Medicine/Division Hematology/Oncology and ⁵Department of Biochemistry and Molecular Genetics, Northwestern University, Chicago, IL 60611, USA, ²Cellular Screening Center, Institute for Genomics & Systems Biology, The University of Chicago, Chicago, IL 60637, USA, ³Laboratory of Muscle Stem Cells and Gene Regulation, NIAMS, NIH, Bethesda, MD 20892, USA, ⁴DigiPen Institute of Technology, Redmond, WA 98052, USA,

⁶ Authors share first authorship

Corresponding author: Marcus E. Peter, E-mail: m-peter@northwestern.edu, phone: 312-503-1291; FAX: 312-503-0189.

Keywords: RNAi, miRNAs, strand selection, toxicity, evolution

32 SUMMARY

33 Many small interfering (si)RNAs are toxic to cancer cells through a 6mer seed sequence (position 2-7 of the
34 guide strand). A siRNA screen with all 4096 possible 6mer seed sequences in a neutral siRNA backbone
35 revealed a preference for guanine in positions 1 and 2 and a high overall G or C content in the seed of the
36 most toxic siRNAs for four tested human and mouse cell lines. Toxicity of these siRNAs stems from
37 targeting survival genes with C-rich 3'UTRs. The master tumor suppressor miRNA miR-34a-5p is toxic
38 through such a G-rich 6mer seed and is upregulated in cells subjected to genotoxic stress. In the absence of
39 most canonical miRNAs, a modified highly toxic form of miR-320a-3p is induced. An analysis of all mature
40 miRNAs suggests that during evolution most miRNAs evolved to avoid guanine at the 5' end of the 6mer
41 seed sequence of the guide strand. In contrast, for certain tumor suppressive miRNAs the guide strand
42 contains a G-rich toxic 6mer seed, presumably to eliminate cancer cells.

43

44 INTRODUCTION

45 RNA interference (RNAi) is a form of post-transcriptional regulation exerted by 19-21 nt long double
46 stranded RNAs that negatively regulate gene expression at the mRNA level. RNAi-active guide RNAs can
47 come from endogenous siRNAs and micro(mi)RNAs. For a miRNA, the RNAi pathway begins in the
48 nucleus with transcription of a primary miRNA precursor (pri-miRNA) ¹. Pri-miRNAs are first processed by
49 the Drosha/DGCR8 microprocessor complex into pre-microRNAs ², which are then exported from the
50 nucleus to the cytoplasm by Exportin 5 ³. Once in the cytoplasm, Dicer processes them further ^{4,5} and these
51 mature dsRNA duplexes are then loaded into Argonaute (Ago) proteins to form the RNA-induced silencing
52 complex (RISC) ⁶. The sense/passenger strand is ejected/degraded, while the guide strand remains associated
53 with the RISC ⁷. Depending on the degree of complementarity between the guide strand and its target, the
54 outcome of RNAi can either be target degradation - most often achieved by siRNAs with full
55 complementarity to its target mRNA ⁸ - or miRNA-like cleavage-independent silencing, mediated by
56 deadenylation/degradation or translational repression ⁹. The latter mechanism can be initiated with as little as
57 six nucleotide base-pairing between a guide RNA's so-called seed sequence (positions 2 to 7) and fully
58 complementary seed matches in the target RNA ^{10,11}. This seed-based targeting most often occurs in the
59 3'UTR of a target mRNA ^{12,13}.

60 A number of miRNAs function either as tumor suppressors or as oncogenes ¹⁴. Their cancer specific
61 activities are usually explained by their identified targets, being oncogenes tumor or suppressors,
62 respectively ¹⁴. Examples of targets of tumor-suppressive miRNAs are the oncogenes Bcl-2 for miR-15/16 ¹⁵
63 and c-Myc for miR-34a ¹⁶. While many miRNAs have been reported to have both tumor suppressive and
64 oncogenic activities depending on the cancer context, examples for widely established tumor promoting
65 miRNAs are miR-221/222, miR-21, miR-155, and members of the miR-17~92 cluster, or its paralogues

66 miR-106b~25 and miR-106a~363^{17,18}. In contrast, two of the major tumor suppressive miRNA families are
67 miR-15/16 and the p53 regulated miR-34a/c and miR-34b¹⁹.

68 We recently discovered that many si- and shRNAs can kill all tested cancer cell lines through RNAi by
69 targeting the 3'UTRs of critical survival genes²⁰. Cancer cells have difficulty developing resistance to this
70 mechanism both *in vitro* and when treated *in vivo*²¹. We reported that a 6mer seed sequence in the toxic
71 siRNAs is sufficient for effective killing²⁰. We have now performed a strand specific siRNA screen with a
72 library of individual siRNAs representing all 4096 possible 6mer seed sequences in a neutral RNA duplex.
73 This screen, while based on siRNA biochemistry was not designed to identify targets that are degraded
74 through siRNA mediated slicing activity but to identify toxicity caused by moderately targeting hundreds of
75 genes required for cell survival in a mechanism similar to miRNA-induced silencing.

76 We report that the most toxic 6mer seeds are G-rich with a G enrichment towards the 5' end targeting
77 survival genes with a high C content in their 3'UTR in a miRNA-like manner. Many tumor suppressive
78 miRNAs such as miR-34a-5p but none of the established oncogenic miRNAs contain G-rich 6mer seeds and
79 most of miR-34a-5p's toxicity comes from its 6mer seed sequence. Mature miRNAs from older and more
80 conserved miRNAs contain less toxic seeds. We demonstrate that for most miRNAs the more abundant
81 mature form corresponds to the arm that contains the less toxic seed. In contrast, for major tumor suppressive
82 miRNAs, the mature miRNA is derived from the arm that harbors the more toxic seed. Our data allow us to
83 conclude that while most miRNAs have evolved to avoid targeting survival and housekeeping genes, certain
84 tumor suppressive miRNAs function to kill cancer cells through a toxic G-rich 6mer seed targeting the
85 3'UTR of survival genes.

86

87 **RESULTS**

88 **Identifying the most toxic 6mer seeds**

89 To test how certain 6mer seeds present in the guide strand of a siRNA affect cancer cell survival, we recently
90 designed a neutral 19mer oligonucleotide scaffold with two nucleotide 3' overhangs, and we demonstrated
91 that modifying a siRNA strand at positions 1 and 2 by 2'-O-methylation (OMe) completely blocks its loading
92 into the RISC²². Different 6mer sequences can be inserted at positions 2-7 of the guide strand with the
93 designated passenger strand modified by OMe (two red Xs in **Fig. 1a**). Transfection efficiency and
94 conditions were optimized for each cell line used. To determine the general rules of seed-based toxicity, we
95 individually transfected 4096 siRNAs with all possible 6mer seed sequences in this 19mer scaffold into two
96 human, HeyA8 (ovarian cancer) and H460 (lung cancer), and two mouse cell lines M565 (liver cancer) and
97 3LL (lung cancer). This allowed us to rank all 4096 6mer seeds according to their toxicity (**Fig. 1b**,
98 **Supplementary Table 1**, and **6merdb.org**). The congruence between the results of the two human cell lines
99 and the two human and two mouse cell lines was quite high ($r=0.68$ and 0.65 , respectively, **Fig. 1c**)

100 suggesting that many siRNAs were toxic through a mechanism independent of cancer origin and species.
101 Toxicity was caused by the different 6mer seeds in the *guide* strand. A siRNA duplex highly toxic to all cell
102 lines (#2733, HeyA8 cell viability = 1.4%) strongly inhibited cell growth and reduced cell viability of
103 HeyA8 cells only when the passenger strand was modified by the OMe modification. Toxicity was
104 completely blocked when the guide strand was modified (**Fig. S1a**). The toxicity was due to RNAi as
105 knockdown of AGO2 abolished the toxicity of two of the most toxic siRNAs (**Fig. S1b**).

106 We previously reported that the CD95 ligand (CD95L) coding region (CDS) is enriched in sequences that
107 when converted into si- or shRNAs are toxic to cancer cells²⁰ and that the CD95L mRNA itself is toxic to
108 cells²³. We now report a substantial correlation between the most toxic CD95L-derived shRNAs and the
109 toxicity of their predicted 6mer seed (**Fig. 1d**) suggesting the CD95L-derived si/shRNAs kill cancer cells
110 through 6mer seed toxicity. Consistent with this assumption we found that the 6mer seeds of 4 previously
111 tested siRNAs derived from CD95L²⁴ in this screen were about as toxic as the full length siRNAs, with
112 siL3^{Seed} being the most toxic followed by siL2^{Seed} and less or no toxicity associated with siL4^{Seed} and siL1^{Seed}
113 (**Fig. 1b, Fig. 1c**). Our recent analysis suggested that the toxic si/shRNAs act like artificial miRNAs by
114 targeting the 3'UTR of mRNAs²⁰.

115

116 **6mer seeds enriched in G at the 5' end are most toxic to human and mouse cell lines**

117 We noticed that the 6mer seeds in siL3 and siL2 have a higher G content than the ones in siL4 and siL1 (**Fig.**
118 **1b**). By analyzing the screen results of all four cell lines (**Fig. S2**), we found that a high G content of the seed
119 correlated better with toxicity than a high C content. Almost no toxicity was found with seeds with a high A
120 content. To test the effect of nucleotide content on toxicity directly, we retested the 19 seed duplexes with
121 the highest content (>80%) for each of the four nucleotides in the four cell lines (**Fig. 2**). The reanalysis also
122 allowed us to determine the reproducibility of the results obtained in the large screens (which for technical
123 reasons had to be performed in three sets). All data on the three cell lines were highly reproducible especially
124 for the most toxic seeds (**Fig. S3a**). When the data on the four cell lines were compared, it became apparent
125 that in all cell lines, the G-rich seeds were by far the most toxic followed by the C-rich, U-rich, and A-rich
126 seeds (**Fig. 2a**). This indicates it is mostly the G content that determines toxicity.

127 Most genome-wide siRNA libraries designed to study functions of individual genes are highly
128 underrepresented in G and C to increase RNAi specificity²⁵ (**Fig. S3b**, left panel). In contrast, our complete
129 set of 6mer seed duplexes exhibits no nucleotide composition bias, allowing us to test the contributions of all
130 four nucleotides in each of the 6 seed positions (**Fig. S3b**, right panel). To determine the nucleotide content
131 of the most toxic seeds, we averaged the nucleotide content at each of the 6 positions of either the 200 most
132 or 200 least toxic seed duplexes for each of the two human and the two mouse cells (**Fig. 2b**,
133 **Supplementary Table 1**). In all four cell lines, we found that a high G content towards the 5' end of the seed

134 and a C in position 6 was most toxic (**Fig. 2b** and **Fig. S3c**). In contrast, non-toxic seeds were A and U-rich
135 especially when positioned at the 5' end. While the rules of toxicity that emerged are almost identical
136 between human and mouse, we noticed a subtle difference. C-rich 6mer seeds are slightly more toxic to
137 mouse than to human cells. This can be seen in the nucleotide composition of the most toxic seeds (**Fig. 2b**),
138 a slightly higher toxicity of the most C rich seeds in the siRNA retest (**Fig. 2a**), and this can also be explored
139 at 6merdb.org.

140

141 **siRNAs with toxic seeds target housekeeping genes enriched in C-rich sequences in their 3'UTR**

142 We previously showed that si- and shRNAs are toxic through 6mer seed toxicity preferentially targeting
143 hundreds of genes critical for cell survival²⁰. We had developed a Toxicity Index (TI), a simple tool to
144 predict the most toxic seeds based on the ratio of putative seed match occurrences in the 3'UTR of set of
145 survival genes (SGs) versus a set of genes not involved in cell survival (nonSGs). We now compared the TI
146 with our experimentally determined 6mer seed toxicity in the three cell lines screened (**Fig. S4**) and found a
147 significant correlation between these two types of analyses, further supporting the mechanism of toxicity.
148 Knowing that seed sequences rich in G are most toxic suggested the targeted genes carry C-rich seed
149 matches in their 3'UTR. To be most stringent, we used a list of the 20 6mer seed containing siRNAs that
150 were most toxic to both HeyA8 and H460 cells (**Supplementary Table 2**). The G richness towards the 5'
151 end of the 6mers in these toxic seeds and the 5' A/U richness of the nontoxic seeds was even more
152 pronounced than in the top/bottom 200 most toxic seeds (**Fig. 3a**). We scored for the occurrence of seed
153 matches to the 20 seeds in each group in the 3'UTR, the CDS and the 5'UTR of a set of 938 critical SGs
154 similar to one recently described²⁰ and an expression-matched set of 938 nonSGs. We found a significantly
155 higher count ratio of toxic versus nontoxic seed matches in the 3'UTR of SGs when compared to nonSGs
156 (**Fig. 3b**, right panel). Consistent with a miRNA-like function no such enrichment was found when the CDS
157 was analyzed (**Fig. 3b**, center panel). An inverse ratio of sequences complementary to the 6mer seeds of
158 unknown significance was found in the 5'UTR (**Fig. 3b**, left panel). This result was very similar when we
159 scored for seed matches to the 100 seeds most toxic and least toxic to both human cell lines (**Fig. S5a**). An
160 enrichment of the exact seed matches in 3'UTRs was consistent with the overall higher C content of 3'UTRs
161 of SGs when compared to nonSGs (different peak maxima in **Fig. 3c**). A metaplot analysis of the 500 bases
162 upstream and downstream of the translational start and stop site of all human genes showed that as expected
163 the 3'UTR was enriched in A and U (**Fig. 3d**, top). Interestingly, SGs had a lower A/U content in a region
164 ~150-500 bases into the 3'UTR than expression matched nonSGs (**Fig. 3d**, green horizontal bar, center and
165 bottom). To determine where survival genes are being targeted by toxic seed containing siRNAs we again
166 performed a metaplot analysis this time plotting the locations of seed matches to the 20 6mer seeds that were
167 most and least toxic to both human cell lines (**Fig. 3e**, an analysis with the 100 most/least toxic seeds is

168 provided in **Fig. S5b**). When analyzing all human coding genes we found the reverse complements of the
169 most toxic seeds to be highly enriched at the beginning of the 3'UTR whereas the reverse complements of the
170 least toxic seeds were underrepresented in this region (**Fig. 3e**, top). This effect was not due to a much higher
171 G/C or lower A/U content in this region (**Fig. 3d**, top). A comparison of the location of these seed matches in
172 the SGs and in expression matched nonSGs confirmed this general trend, however, two differences between
173 SGs and nonSGs became apparent: 1) nonSGs have more nontoxic seed matches ~150-500 bases into the
174 3'UTR (**Fig. 3e**, bottom, green horizontal bar) maybe due to the higher A/U content of this region (**Fig. 3d**,
175 center and bottom). 2) SGs contain a small stretch at positions 42-65 into the 3'UTR (**Fig. 3e** and **Fig. S5b**,
176 center, red horizontal bar) that is enriched in seed matches for the most toxic seeds. This region in SGs seems
177 to be a preferential target site for siRNAs carrying toxic G-rich seed sequences.

178

179 **Tumor suppressive miR-34a-5p kills cancer cells through its toxic 6mer seed**

180 The toxic siRNAs kill cancer cells through 6mer seed toxicity by a mechanism reminiscent of the function of
181 miRNAs. To test whether actual miRNAs could kill cancer cells with the help of toxic 6mer seeds, we
182 analyzed the seed toxicity determined in our screen for all known ~2600 mature miRNAs expressed as either
183 the 3p or 5p arm (**6merdb.org**). While none of the 6mer seeds present in the predominant arm (guide strand)
184 of the most oncogenic miRNAs (miR-221/222, miR-21, miR-155, the miR-17~92, miR-106b~25, and miR-
185 106a~36 clusters) were toxic (reduced viability >50%, stippled line in **Fig. 4a**), two of the major tumor
186 suppressive miRNA families, miR-15/16 and p53 regulated miR-34a/c and miR-34b contained toxic seeds in
187 the guide strand (**Fig. 4a**). This suggested these two families were killing cancer cells through toxic 6mer
188 seeds. Interestingly, two other major tumor suppressive families, let-7 and miR-200, did not contain toxic G-
189 rich seeds in their guide strand, suggesting they may be tumor suppressive through other mechanisms, such
190 as inducing and maintaining cell differentiation²⁶.

191 When transfecting the pre-miRs of miR-34a-5p, miR-15a-5p and let-7a-5p into HeyA8 cells, the potency
192 of these three miRNAs to reduce cell growth mimicked the toxicity of their 6mer seed containing siRNAs
193 (**Fig. 4b** and **4a**). This suggested that a large part of their toxicity comes from the composition of the seed
194 position 2-7. The most toxic seed in a major tumor suppressive miRNA was present in miR-34a5p/34c-5p, a
195 master regulator of tumor suppression²⁷. We directly compared the toxicity of pre-miR-34a-5p and its toxic
196 seed in the neutral scaffold with blocked passenger strand (si34a-5p^{Seed}) in the same assays (**Fig. 4c**).
197 Strikingly, the toxicity evoked by these two RNA species (assessed by growth inhibition and DNA
198 fragmentation) was similar. Cells showed the typical morphology we found in cells dying from toxic siRNAs
199 (**Fig. 4d**)^{20,24,28}. To determine the contribution of the 6mer seed sequence of miR-34a-5p to its toxicity and
200 the mode of cell death, we performed a RNA-Seq analysis on HeyA8 cells transfected with either miR-34a-
201 5p or si34a-5p^{Seed} (**Fig. 4e**, top) (**Supplementary Table 3**). The vast majority of genes were significantly up-

202 and downregulated by both RNA duplexes (**Fig. 4e**, bottom). While miR-34a-5p targeted a subset of genes
203 not affected by miR-34a-5p^{Seed}, the majority of genes (>78%) were downregulated >1.5 fold by both the
204 premiR and the 6mer seed duplex (**Fig. 4f**, left). A Sylamer analysis is a unbiased approach allowing to
205 identify which seed matches are enriched in the 3'UTRs of downregulated genes from RNAseq data ²⁹. In
206 this analysis both duplexes caused similar and highly effective downregulation of the mRNAs that carry a
207 6mer seed match (**Fig. 4g**). When the Sylamer analysis was performed with either 7mer or 8mer seeds,
208 enrichment of seed matches was much less significant (**Fig. S6a**) suggesting that most of the targeting by
209 both RNAs only required a 6mer seed.

210 Consistent with this activity, targeting by both RNA duplexes resulted in a very similar reduction of
211 survival genes (**Fig. 4h**). The genes downregulated by both the premiR and the 6mer seed construct were
212 highly enriched in genes involved in regulation of cell cycle, cell division, DNA repair, and nucleosome
213 assembly (**Fig. 4f**, right). These GO terms were very similar to the ones we found enriched in downregulated
214 genes in cells dying after transfection with CD95R/L-derived si/shRNAs containing toxic 6mer seeds ²⁰. In
215 contrast, no such GO terms were found enriched when the same analysis was performed with the upregulated
216 genes as control (**Fig. S6b**). While both miR-34-5p and si34a-5p^{Seed} caused the most significant
217 downregulation of genes carrying 8mers in their 3'UTR (**Fig. S6c**), only the most highly downregulated
218 genes that carry the shared 6mer seed match were grouped in a number of GO terms that are consistent with
219 6mer seed toxicity as previously reported ²⁰ and barely any GO terms were shared among genes that
220 contained 7 or 8mer seed matches (**Fig. S6d**). All these data suggest that miR-34a-5p kills cancer cells using
221 its toxic 6mer seed. While optimal miRNA targeting requires at least a 7mer seed interaction and also
222 involves nucleotides at positions 13-16 of the miRNA ³⁰, the cell death inducing activity of this tumor
223 suppressive miRNA may only require the 6mer seed.

224 225 **Toxic 6mer seed toxicity is shaping the miRNA repertoire**

226 Toxic 6mer seeds may be a driving force in miRNA evolution, whereby toxic seed sequences are either
227 selected against - because they contribute to cell toxicity - or are preserved to operate as tumor suppressors.
228 Based on the composition of toxic 6mer seeds and the enrichment of corresponding seed matches in survival
229 genes, we could now ask whether and when miRNAs that contain toxic G-rich sequences in positions 2-7 of
230 their seeds evolved. When comparing all mature miRNA arms annotated in TargetScan Human 7, we noticed
231 that miRNAs in highly conserved miRNA seed families contained 6mer seed sequences that were much less
232 toxic in our screen than seeds in poorly conserved miRNAs (**Fig. 5a**, left panel and **Fig. S7a**). Weakly
233 conserved miRNA seed families would be expected to be younger in evolutionary age than highly conserved
234 ones. Consistent with this assumption we found that the 6mer seeds of younger miRNAs (<10 million years
235 old) were more likely to be toxic to cells than the ones of older miRNAs (>800 million years old) ³¹ (**Fig. 5a**,

236 right panel and **Fig. S7b**). Most importantly, when comparing miRNAs of different ages, it became
237 apparent that seeds of miRNAs over the last 800 million years were gradually depleted of G beginning at the
238 5' end and eventually also affecting positions 3-5 until the oldest ones, where A and U had replaced G as the
239 most abundant nucleotide in all six positions (**Fig. 5b**). These analyses indicated that most highly conserved
240 miRNAs avoid G in potentially toxic seed positions. Interestingly, the most toxic seed sequences were found
241 in miRtrons (**Fig. 5c** and **Fig. S7c**), miRNAs that are derived by splicing short introns ³².

242 miRNAs are expressed as pre-miRs and usually only one major species of mature miRNA (either the 5p
243 or the 3p arm) is significantly expressed in cells produced from one of the two strands of the premiR stem ³³.
244 Consistent with the assumption that cells cannot tolerate toxic 6mer seeds, we now tested across 780
245 miRNAs which have been shown to give rise to both a 3p and a 5p arm whether the more highly expressed
246 arm contains a seed of lower toxicity than the lesser expressed arm (**Fig. 5d**). We ranked the miRNAs
247 according to the ratio of the 6mer seed toxicity associated with the guide arm to the lesser-expressed arm
248 (**Supplementary Table 4**). When we labeled the major tumor suppressive and oncogenic miRNAs, we
249 noticed the highly expressed arm of most of the oncogenic miRNAs contained a 6mer seed that was not toxic
250 in our screen (**Fig. 5d**, green dots). In contrast, for most of the tumor suppressive miRNAs, the dominant arm
251 contained a seed much more toxic than the lesser arm (**Fig. 5d**, red dots). The overall difference in ratio
252 between the two groups of miRNAs was highly significant. A more detailed analysis of these data revealed
253 that the three oncogenic miRNAs with the highest ratio in toxicity between their arms, miR-363, miR-92a-2,
254 and miR-25, were almost exclusively expressed as the non-toxic 3p form (**Fig. 5e**, top). In contrast, the
255 dominant arm of the three tumor suppressive miRNAs, miR-34a, miR-34c, and miR-449b contained the
256 most toxic seed sequence (**Fig. 5e**, bottom). Interestingly, miR-449b has the same seed sequence as miR-34a
257 and has been suggested to act as a backup miRNA for miR-34a ³⁴. These data are consistent with most tumor
258 suppressive miRNAs using 6mer seed toxicity to kill cancer cells and suggest that this mechanism developed
259 over hundreds of millions of years.

260

261 **Genotoxic drugs upregulate toxic 6mer seed containing miRNAs**

262 Our data showing that miR-34a-5p contains a toxic 6mer seed, along with miR-34a being upregulated after
263 genotoxic stress ¹⁹, led us to wonder whether miR-34a-5p would contribute to cell death induced by
264 genotoxic drugs and whether this type of cell death had similarities to the death observed in cells dying from
265 toxic 6mer seed containing si/shRNAs. This would be consistent with the observation that many genotoxic
266 drugs induce multiple cell death pathways ^{35,36,37,38,39}. To compare cell death induced by different genotoxic
267 agents with that of toxic si/shRNAs, we treated the p53 wild-type ovarian cancer cell line HeyA8 with
268 doxorubicin (Doxo), carboplatin (Carbo), or etoposide (Eto) and performed a RNA-Seq analysis. Drug
269 concentrations were chosen so that after 80 hrs, treatment would slow down cell growth and induce signs of

270 stress without major cell death occurring to capture changes that could be causing cell death rather than
271 being the result of it (**Fig. S8a** and data not shown). The morphological changes in the cells treated with the
272 drugs were very similar to the ones seen in cells treated with si/shRNAs (**Fig. S8b**), and similar to reported
273 morphologies of cells treated with genotoxic drugs^{40,41}.

274 The ranked lists of downregulated RNAs isolated from HeyA8 cells treated with the three drugs were
275 subjected to a gene set enrichment analysis (GSEA) to determine whether survival genes were enriched in
276 the downregulated genes (**Fig. S9a**). There was strong enrichment of downregulated survival genes towards
277 the top of the ranked list. 102 of the survival genes were downregulated in cells treated with any of the three
278 drugs (**Fig. S9b**). In a DAVID gene ontology analysis, these genes were strongly enriched in clusters
279 involved in chromosome segregation, DNA replication, cell cycle regulation, and mitosis, typical for 6mer
280 seed toxicity induced cell death (**Supplementary Table 5**). We quantified 30 of the 102 survival genes in
281 HeyA8 cells treated with Doxo at different time points using an arrayed quantitative PCR (**Fig. S9c**). 24 of
282 the 30 genes' mRNAs were significantly downregulated as early as 7 hours after treatment with no further
283 reduction beyond 15 hrs after treatment, suggesting that their repression was the cause of cell death rather
284 than a consequence. A Metascape analysis of all RNA-Seq data of downregulated RNAs in response to the
285 toxic siL3, si34a-5p^{Seed}, miR-34a-5p, and the three genotoxic drugs suggested a common mode of action
286 (**Fig. S9d**). The GO clusters that were most significantly downregulated in all data sets were again related to
287 DNA repair, cell cycle, and mitosis as described before²⁴.

288 To test whether treatment of cells with genotoxic drugs results in loading the RISC with toxic miRNAs,
289 HeyA8 cells were treated with Doxo for 0, 20, 40 and 80 hrs and all 4 Ago proteins were pulled down using
290 a GW182 peptide⁴². Interestingly, while the amount of AGO2 pulled down was the same at all time points,
291 the amount of bound miRNA-sized RNAs substantially increased with longer treatment times (**Fig. 6a**). This
292 was most likely the result of an overall increase in total small RNAs in the treated cells (**Fig. 6b**).
293 Alternatively, this could also be a result of cells dividing more slowly and a stable RISC. After Doxo
294 treatment, >99% of the Ago-bound small RNAs were miRNAs (data not shown). miR-34a/b/c-5p bound to
295 Ago proteins were upregulated at all time points (**Fig. S10a**). To determine the contribution of miR-34a-5p
296 and other miRNAs to the toxicity seen in cells exposed to the genotoxic drugs, we treated Drosha k.o. cells -
297 devoid of most canonical miRNAs⁴³ - with the three genotoxic drugs (**Fig. S11**). These cells were
298 hypersensitive to the toxicity induced by any of the three drugs. We attributed this response to the absence of
299 most canonical miRNAs that protect cells from toxic RNAi active sequences²⁰. This result also suggested
300 involvement of small RNAs that do not require Drosha for processing. As expected, the composition of small
301 RNAs bound to Ago proteins dramatically varied between wild-type and Drosha k.o. cells (**Fig. 6c**). In the
302 absence of most canonical miRNAs, miR-320a-3p, which was previously shown not to require Drosha for its
303 biogenesis⁴³, represented more than 86% of all Ago-bound miRNAs. Similar to HeyA8 cells (see **Fig. S10a**),

304 Ago-bound miR-34a-5p was upregulated in wild-type but not in Drosha k.o. HCT116 cells upon Doxo
305 treatment (**Fig. S10b**, right). Interestingly, the average 6mer seed toxicity of all Ago-bound miRNAs >1.5
306 fold upregulated in HCT116 wt cells was significantly higher than the ones >1.5 fold downregulated in cells
307 treated with Doxo (**Fig. 6d**, left). While in the Drosha k.o. cells, a number of nontoxic miRNAs were
308 downregulated, the only miRNA that was upregulated in the RISC (1.49 fold) was miR-320a-3p (**Fig. 6d**,
309 right). However, upon closer inspection it became clear that this form of miR-320a-3p was shortened by two
310 nucleotides at the 5' end. This resulted in the shift of the 6mer seed into a G-rich sequence (**Fig. 6d**, right),
311 converting a moderately toxic miRNA (average viability = 49.2%) into a highly toxic one (average viability
312 = 9.3%, **Fig. 1b**). To test this predicted increase in toxicity experimentally, we transfected HeyA8 cells with
313 either the authentic pre-miR-320a-3p or a miR-320a-3p^{Seed} duplex that corresponded to the shifted Ago-
314 bound miR-320a-3p sequence (miR-320a-3p^{Ago}) (**Fig. 6e**). While pre-miR-320a-3p was not toxic, miR-320a-
315 3p^{Ago} completely blocked the growth of the cells. Toxicity of miR-320a-3p^{Ago} was established in four human
316 and mouse cell lines (**Fig. 6f**). These data suggested that in the absence of other miRNAs that could kill cells
317 through 6mer seed toxicity, miR-320a-3p (and possibly other small RNAs) may represent an alternative
318 mechanism that ensures that genotoxic stressors can kill cells with defective miRNA processing often
319 observed in cancer^{44,45}. In summary, our data suggest that certain tumor suppressive miRNAs, such as miR-
320 34a-5p and miR-320a-3p exert their tumor suppressive activities by carrying toxic 6mer seed sequences that
321 can kill cancer cells by targeting survival genes in C-rich regions close to the start of their 3'UTR. This
322 activity may contribute to the cell death induced by genotoxic drugs.

323

324 DISCUSSION

325

326 We previously discovered a fundamental cell type- and species-independent form of toxicity that is evoked
327 by the 6mer seed sequence in si-/shRNAs that function similar to miRNAs²⁰. We have now performed an
328 siRNA screen that effectively tested the miRNA activities of all 4096 different 6mer seed sequences.
329 Performing the screen in four cell lines (two human and two mouse) ensured that the results were relatively
330 independent of species or cell type specific transcriptomes. The screen has discovered the rules underlying
331 this seed toxicity and allows prediction of the 6mer seed toxicity for any siRNA, shRNA, miRNA with a
332 known 6mer seed (<https://6merdb.org>).

333

334 Based on this screen, the toxicity of a number of tumor suppressive miRNAs could be predicted solely
335 on the basis of their 6mer seed sequences. The enrichment of G in the first 2-3 positions of the most toxic
336 seeds is consistent with the way Ago proteins scan mRNAs as targets. This involves mainly the first few
337 nucleotides (positions 1-3) of the seed⁴⁶. miR-34a-5p contains two Gs in positions 1 and 2 of its 6mer seed.
While miR-34a-5p is considered a master tumor suppressive miRNA, no single target has been identified to

338 be responsible for this activity. Over 700 targets implicated in cancer cell proliferation, survival, and
339 resistance to therapy have been described¹⁶. Our data now suggest that miR-34a-5p uses 6mer seed toxicity
340 to target hundreds of housekeeping genes. Our data provide the means to rationally design new artificial
341 miRNAs as anti-cancer reagents that attack networks of survival genes. In humans, miR-34a is highly
342 expressed in many tissues. Consistent with our data that delivering siRNAs with toxic 6mer seeds to mice are
343 not toxic to normal cells²¹ miR-34a exhibits low toxicity to normal cells *in vitro* and *in vivo*⁴⁷. miR-34a
344 (MRX34) became the first miRNA to be tested in a phase I clinical trial of unresectable primary liver cancer
345^{27,48}. The study was recently terminated and reported immune-related adverse effects in several individuals. It
346 was suggested that these adverse effects may have been caused by either a reaction to the liposome-based
347 carrier or the use of double-stranded RNA¹⁶. In addition, they may be due to an undesired gene modulation
348 by miR-34a itself defined by sequences outside the 6mer seed¹⁶. Our data suggest that miR-34a exerts
349 toxicity mostly through the 6mer seed of its 5p arm and that its 700 known targets may be part of the
350 network of survival genes that are targeted. The comparison of the RNA-Seq data of cells treated with either
351 miR-34a-5p or si34-5p^{Seed} now allows to determine whether these two activities can be separated.

352 Our data provide evidence that genotoxic drugs kill cancer cells, at least in part, by triggering the toxic
353 6mer seed mechanism. Exposure of cancer cells to such drugs resulted in upregulation of tumor suppressive
354 miRNAs, most prominently of the p53 regulated miR-34 family¹⁹. While one report demonstrated that
355 inhibiting miR-34a rendered cancer cells more resistant to cell death induced by genotoxic stress⁴⁹, another
356 one found no effect of knocking out miR-34a on the sensitivity of HCT116 or MCF-7 cells to Doxo⁵⁰. This
357 mechanism may be highly redundant and may involve many miRNAs. Our analysis of Ago-bound miRNAs
358 in Drosha k.o. cells suggest that in the absence of miR-34a, the noncanonical miR-320a-3p which was
359 recently also found to be p53 regulated⁵¹ may act as a backup miRNA that can still respond to genotoxic
360 stress in case the amounts of other miRNAs are reduced, for instance in cases of mutations in miRNA
361 biogenesis associated genes frequently found in human cancers⁴⁴. In addition, recent data suggest that other
362 toxic small RNAs can also be taken up by the RISC and negatively regulate cell growth through their toxic
363 6mer seed (data not shown).

364 It was shown before that miRNAs overall avoid seed sequences that target the 3'UTR of
365 survival/housekeeping genes^{52, 53}. Survival genes therefore are depleted in seed matches for the most
366 abundant miRNAs in a cell. That also means 3'UTRs of survival genes must be enriched in sequences not
367 targeted by the seeds present in most miRNAs. Our combined data now suggest it is these sequences that
368 toxic siRNAs and tumor suppressive miRNAs with toxic 6mer seeds are targeting. Our analyses also suggest
369 that most miRNAs have evolved over the last 800 million years by gradually depleting G in their seeds
370 beginning at the 5' end. In addition, the most abundant miRNAs have evolved to use the arm with the lower
371 6mer seed toxicity as the active guide strand, presumably to avoid killing cells. Only in a minority of tumor-

372 suppressive miRNAs does the dominant guide strand contain a toxic seed. By ranking miRNAs according
373 to whether they express the arm with the seed of higher toxicity, it is now possible to identify novel tumor
374 suppressive miRNAs (see 6merdb.org).

375 In summary, we have determined the rules of RNAi targeting by toxic 6mer seeds. These rules allowed
376 us to predict with some confidence which si/shRNAs or miRNAs have the potential to kill cells through their
377 toxic 6mer seed. Toxic miRNAs seem to be involved in killing cancer cells in response to genotoxic drugs.
378 Toxic 6mer seeds are present in a number of tumor-suppressive miRNAs that can kill cancer cells. Our data
379 allow new insights into the evolution of miRNAs and provide evidence that 6mer seed toxicity is shaping the
380 miRNA repertoire.

381

382 **METHODS**

383 **Reagents, cell lines and antibodies**

384 HeyA8 (RRID:CVCL_8878) and H460 (ATCC HTB-177) cells were cultured in RPMI1640 medium
385 (Cellgro Cat#10-040) supplemented with 10% FBS (Sigma Cat#14009C) and 1% L-Glutamine (Corning
386 Cat#25-005). 3LL cells (ATCC CRL-1642) were cultured in DMEM medium (Gibco Cat#12430054)
387 supplemented with 10% FBS and 1% L-Glutamine. Mouse hepatocellular carcinoma cells M565 were
388 previously described⁵⁴ and cultured in DMEM/F12 (Gibco Cat#11330) supplemented with 10% FBS, 1% L-
389 Glutamine and ITS (Corning #25-800-CR). HCT116 parental (Cat#HC19023, RRID:CVCL_0291) and the
390 Drosha k.o. clone (clone #40, Cat#HC19020) were purchased from Korean Collection for Type Cultures
391 (KCTC). Both HCT116 cell lines were cultured in McCoy's 5A medium (ATCC, Cat#30-2007)
392 supplemented with 10% FBS and 1% L-Glutamine. All cell lines were authenticated by STR profiling. Anti-
393 Argonaute-2 antibody (cat#ab186733) was purchased from Abcam, anti- β -actin antibody from Santa Cruz
394 (#sc-47778), and secondary antibody for Western blot was Goat anti-rabbit, IgG-HRP from Southern
395 Biotech (#SB-4030-05). Etoposide (Cat#BML-GR307-0100) was purchased from Enzo Life Sciences,
396 propidium iodide (#P4864) doxorubicin (Cat#D1515) and carboplatin (Cat#C2538) were from Sigma-
397 Aldrich.

398

399 **siRNA screens and cell viability assay**

400 The non-toxic siRNA backbone used in the 4096 screen was designed as previously described²². Briefly, the
401 siNT2 sequence was used as a starting point and four positions in the center of siNT2 were replaced with the
402 complementary nucleotides in order to remove any identity between the backbone siRNA and the toxic siL3
403 while retaining the same GC content. Two 2'-O-methylation groups were added to positions 1 and 2 of the
404 passenger strand to prevent loading into the RISC. The 6mer seed region (position 2-7 on the guide strand)
405 was then replaced with one of the 4096 possible seeds. Transfection efficiency was optimized for each of the

406 four cell lines individually. For HeyA8 and M565 cells, the reverse transfection and the quantification of
407 cellular ATP content in the 4096 seed duplexes screen was done as previously described ²². For 3LL and
408 H460 cells screens were done in a very similar manner except for the amount of RNAiMAX and the number
409 of cells plated. For 3LL cells, 150 cells per well were added in a 384 well plate and 9.3 µl of Lipofectamine
410 RNAiMax was mixed with 990.7 µl of Opti-MEM. For H460 cells, 420 cells per well in a 384 well plate was
411 added and 7.3 µl of Lipofectamine RNAiMax was mixed with 993.7 µl of Opti-MEM.

412

413 **Transfection with short oligonucleotides**

414 For IncuCyte experiments, HeyA8 cells were plated in 50 µl antibiotic free medium in a 96 well plate at
415 1000 cells/well, and 50 µl transfection mix with 0.1 µl RNAiMAX and siRNAs or miRNA precursors were
416 added during the plating. For the AGO2 knockdown experiment, 100,000 cells/well HeyA8 cells were
417 reverse-transfected in six-well plates with either non-targeting (Dharmacon, cat#D-001810-10-05) or an
418 AGO2 targeting siRNA SMARTpool (Dharmacon, cat#L004639-00-005) at 25 nM. 1 µl RNAiMAX per
419 well was used for HeyA8 cells. Twenty-four hours after transfection with the SMARTpools, cells were
420 reversed-transfected in a 96-well plate with siNT2, si2733, or si2733 (see **Supplementary Table 1**) at 10
421 nM and monitored in the IncuCyte Zoom. 48 hours after transfection, cells were lysed in RIPA buffer for
422 Western blot analysis as previously described ²².

423 All custom siRNA oligonucleotides were ordered from integrated DNA technologies (IDT) and annealed
424 according to the manufacturer's instructions. In addition to the 4096 siRNAs of the screen the following
425 siRNA sequences were used:

426 siNT1 sense: rUrGrGrUrUrUrArCrArUrGrUrCrGrArCrUrArATT;

427 siNT1 antisense: rUrUrArGrUrCrGrArCrArUrGrUrArArArCrCrAAA;

428 siNT2 sense: rUrGrGrUrUrUrArCrArUrGrUrUrGrUrGrUrGrATT;

429 siNT2 antisense: rUrCrArCrArCrArArCrArUrGrUrArArArCrCrAAA;

430 siL3 sense: rGrCrCrCrUrUrCrArArUrUrArCrCrCrArUrArUTT;

431 siL3 antisense: rArUrArUrGrGrGrUrArArUrUrGrArArGrGrGrCAA;

432 si-miR-34a-5p^{Seed} sense: mUmGrGrUrUrUrArCrArUrGrUrArCrUrGrCrCrATT;

433 si-miR-34a-5p^{Seed} antisense: rUrGrGrCrArGrUrArCrArUrGrUrArArArCrCrAAA;

434 miR-320a-3p^{Ago} sense: mCmGrCrCrCrUrCrUrCrArArCrCrCrArGrCrUrUTT

435 miR-320a-3p^{Ago} antisense: rArArGrCrUrGrGrGrUrUrGrArGrArGrGrGrCrGAA.

436 The following miRNA precursors and negative controls were used: hsa-miR-34a-5p (Ambion, Cat. No#
437 PM11030), hsa-let-7a-5p (Ambion, Cat. No# PM10050), hsa-miR-320a-3p (Ambion, Cat. No# PM11621),

438 hsa-miR-15a-5p (Ambion, Cat. No# PM10235), and miRNA precursor negative control #1 (Ambion, Cat.
439 No# AM17110).

440

441 **Monitoring growth over time by IncuCyte and cell death assays**

442 Cells were seeded between 1000 and 3,000 per well in a 96-well plate in triplicates. The plate was then
443 scanned using the IncuCyte ZOOM live-cell imaging system (Essen BioScience). Images were captured
444 every six hours using a 10× objective. Cell confluence was calculated using the IncuCyte ZOOM software
445 (version 2015A). For treatment with genotoxic drugs HeyA8 cells were seeded at 750 cells/well and
446 HCT116 cells were seeded at 3000 cells/well in 96-well plate and treated with one of the three genotoxic
447 drugs (carboplatin, doxorubicin, or etoposide) at various concentrations at the time of plating. Solvent treated
448 (0.025% DMSO in medium) cells were used as control for etoposide. Medium treated cells were used as
449 control for carboplatin and doxorubicin. To assess cell viability, treated cells were subjected to a
450 quantification of nuclear fragmentation or ATP content both as previously described^{20,22}.

451

452 **RNA-Seq analysis**

453 For RNA-Seq data in **Fig. 4e**, 50,000 cells/well HeyA8 cells were reversed transfected in 6-well plates with
454 10 nM of either pre-miR-34a-5p or si-miR-34a-5p^{Seed} with their respective controls. The transfection mix was
455 replaced 24 hours after transfection. Cells were lysed after 48 hours after transfection using Qiazol. For the
456 RNA-Seq data in **Fig. S9**, HeyA8 cells were seeded at 50,000 cells per well in a 6-well plate and treated with
457 three genotoxic drugs in duplicate: carboplatin (25 µg/ml), doxorubicin (50 ng/ml), and etoposide (500 nM).
458 Medium treated cells were used as control for carboplatin and doxorubicin treated cells. Solvent control
459 treated cells (0.025% DMSO in medium) were used as control for etoposide. Cells were lysed after 80 hours
460 drug incubation using Qiazol. Total RNA was isolated using the miRNeasy Mini Kit (Qiagen, Cat.No#
461 74004) following the manufacturer's instructions. An on-column digestion step using the RNase-free
462 DNase Set (Qiagen, Cat.No# 79254) was included for all RNA-Seq samples. The RNA libraries were
463 prepared and sequenced as previously described²⁰ at the Genomics Core facility at the University of
464 Chicago. Reads were aligned to the hg38 version of the human genome, using either Tophat v2.1.0 (RNA-
465 Seq data in **Fig. S9**) or STAR v2.5.2 (RNA-Seq data in **Fig. 4e**). In either case, aligned reads were
466 associated with genes using HTSeq v0.6.1, and the UCSC hg38 transcriptome annotation from
467 iGenomes. Differentially expressed genes were identified using the edgeR R package.

468

469 **Arrayed real-time PCR**

470 The top 30 most downregulated survival genes shared among HeyA8 cells treated with carboplatin,
471 doxorubicin, and etoposide based on the RNA-Seq analysis were selected for a kinetics analysis using real-

472 time PCR. To prepare the RNAs for the kinetics analysis, 75,000/plate HeyA8 cells were plated in 15 cm
473 plate. Twenty-four hours after plating, one plate of HeyA8 cells were lysed in QIAzol as the control sample.
474 The rest of the plates were treated with 50 ng/ml doxorubicin for 7 hrs, 14.5 hrs, and 21 hrs respectively
475 before being lysed in QIAzol. To perform the arrayed real-time PCR, 200 ng total RNA per sample was used
476 as the input to make cDNA using the high-capacity cDNA reverse Transcription Kit (Applied Biosystems
477 #4368814). For TaqMan Low Density Array (TLDA) profiling, custom-designed 384-well TLDA cards
478 (Applied Biosystems, Cat. No#4346799) were selected and used according to the manufacturer's protocols.
479 For each sample, 20 μ l cDNA was mixed with 80 μ l water and 100 μ l TaqMan Universal PCR Master Mix
480 (Applied Biosystems, Cat. No#4304437). A total volume of 100 μ l of each sample is loaded into the 8
481 loading ports on the TLDA card (2 ports for each sample, 4 samples total on one card). The qPCR assays
482 used to detect the 30 genes on the TLDA card are as follows: HIST1H2AI (Hs00361878_s1), CENPA
483 (Hs00156455_m1), HJURP (Hs00251144_m1), FAM72D (Hs00416746_m1), CCNA2 (Hs00996788_m1),
484 KIF20A (Hs00993573_m1), PRC1 (Hs01597839_m1), KIF15 (Hs01085295_m1), BUB1B
485 (Hs01084828_m1), SCD (Hs01682761_m1), AURKA (Hs01582072_m1), NUF2 (Hs00230097_m1),
486 NCAPH (Hs01010752_m1), SPC24 (Hs00699347_m1), KIF11 (Hs00189698_m1), TTK (Hs01009870_m1),
487 PLK4 (Hs00179514_m1), AURKB (Hs00945858_g1), CEP55 (Hs01070181_m1), HMGCS1
488 (Hs00940429_m1), TOP2A (Hs01032137_m1), KIF23 (Hs00370852_m1), INCENP (Hs00934447_m1),
489 CDK1 (Hs00938777_m1), HIST2H2BE (Hs00269023_s1), KNL1 (Hs00538241_m1), NCAPD2
490 (Hs00274505_m1), RACGAP1 (Hs01100049_mH), SPAG5 (Hs00197708_m1), KNTC1 (Hs00938554_m1).
491 GAPDH (Hs99999905_m1) was used as the endogenous control. qPCR assay for individual gene was done
492 in technical triplicates on each TLDA cards. Statistically analysis was performed using Student's t test.

493

494 **Ago affinity peptide purification**

495 The FLAG-GST-T6B WT and mutant peptides was expressed and purified as described ⁴². Briefly,
496 constructs were expressed in BL21-Gold(DE3)pLysS competent cells (Agilent). Bacteria, induced with 1
497 mM Isopropyl β -D-1-thiogalactopyranoside (IPTG), were grown in 1 L overnight at 18°C to OD 0.6. The
498 bacteria were sedimented at 4000g for 15 min and resuspended in 25 ml GST-A buffer (1 mM 4-(2-
499 aminoethyl) benzenesulfonyl fluoride hydrochloride (AEBSF), 1 mM DTT in PBS) supplemented with 1
500 mg/mL lysozyme (Sigma). Samples were sonicated three times for 3 min at 100% amplitude (Sonics,
501 VCX130) and cleared by centrifugation at 20,000g for 20 min. The lysate was loaded onto a column
502 containing 2 ml of bead volume glutathione Sepharose beads (Sigma) and washed two times with GST-A
503 buffer. The GST-tagged protein was eluted in 10 ml of GST-B buffer (20 mM Tris, pH 8.0, and 10 mM
504 glutathione in PBS). The peptide was concentrated using Amicon Ultra-15 Centrifugal Filter Unit (Millipore)
505 and desalted using Zeba Spin Desalting Columns (ThermoFisher).

506

507 **Ago pull down and small RNA-seq**

508 HeyA8 ($5-7 \times 10^6$), HCT116 wild-type ($1.2-1.6 \times 10^8$) or Drosha k.o. ($4.8-6.3 \times 10^7$) cells treated with
509 doxorubicin were lysed in NP40 lysis buffer (20 mM Tris, pH 7.5, 150 mM NaCl, 2 mM EDTA, 1% (v/v)
510 NP40, supplemented with phosphatase inhibitors) on ice for 15 minutes. The lysate was sonicated 3 times for
511 30 s at 60% amplitude (Sonics, VCX130) and cleared by centrifugation at 12,000g for 20 minutes. AGO1-4
512 were pulled down by using 500 μ g of Flag-GST-T6B peptide⁴² and with 60 μ l anti-Flag M2 magnetic beads
513 (Sigma-Aldrich) for 2 hrs at 4°C. The pull-down was washed 3 times in NP40 lysis buffer. During the last
514 wash, 10% of beads were removed and incubated at 95°C for 5 minutes in 2x SDS-PAGE sample buffer.
515 Samples were run on a 4-12% SDS-PAGE and transferred to nitrocellulose membrane. The pull-down
516 efficiency was determined by immunoblotting against AGO2 (Abcam 32381). To the remaining beads 500
517 μ l TRIzol reagent were added and the RNA extracted according to the manufacturer's instructions. The RNA
518 pellet was diluted in 20 μ l of water. The sample was split and half of the sample was dephosphorylated with
519 0.5 U/ μ l of CIP alkaline phosphatase at 37°C for 15 min and subsequently radiolabeled with 0.5 μ Ci γ -³²P-
520 ATP and 1 U/ μ l of T4 PNK kinase for 20 min at 37°C. The AGO1-4 interacting RNAs were visualized on a
521 15% urea-PAGE. The remaining RNA was taken through a small RNA library preparation as previously
522 described⁵⁵. Briefly, RNA was ligated with 3' adenylated adapters and separated on a 15% denaturing urea-
523 PAGE. The RNA corresponding to insert size of 19-35 nt was eluted from the gel, ethanol precipitated
524 followed by 5' adapter ligation. The samples were separated on a 12% Urea-PAGE and extracted from the
525 gel. Reverse transcription was performed using Superscript III reverse transcriptase and the cDNA amplified
526 by PCR. The cDNA was sequenced on Illumina HiSeq 3000.

527 Adapter sequences:

528 Adapter 1 – NNTGACTGTGGAATTCTCGGGTGCCAAGG;

529 Adapter 2 – NNACACTCTGGAATTCTCGGGTGCCAAGG,

530 Adapter 3 – NNACAGAGTGGAATTCTCGGGTGCCAAGG,

531 Adapter 4 – NNGCGATATGGAATTCTCGGGTGCCAAGG,

532 Adapter 47 – NNTCTGTGTGGAATTCTCGGGTGCCAAGG,

533 Adapter 48 – NNCAGCATTGGAATTCTCGGGTGCCAAGG,

534 Adapter 49 – NNATAGTATGGAATTCTCGGGTGCCAAGG,

535 Adapter 50 – NNTCATAGTGGAATTCTCGGGTGCCAAGG.

536 RT primer sequence: GCCTTGGCACCCGAGAATTCCA;

537 PCR primer sequences:

538 CAAGCAGAAGACGGCATAACGAGATCGTGATGTGACTGGAGTTCCTTGGCACCCGAGAATTCCA.

539

540 **Data analyses**

541 GSEA was performed using the GSEA software version 3.0 from the Broad Institute downloaded from
542 <https://software.broadinstitute.org/gsea/>. A ranked list was generated by sorting genes according the
543 Log_{10} (fold downregulation). The Pre-ranked function was used to perform GSEA using the ranked list. 1000
544 permutations were used. Default settings were used. The ~1800 survival genes and ~420 non-survival genes
545 defined previously²⁰ were used as custom gene sets. Default settings were used.

546 The list of survival genes and expression matched non-survival genes were generated by taking the
547 survival and expression matched non-survival genes used previously (20) and retaining only the 938 genes in
548 each group of expression matched survival and non-survival genes with an average expression across all
549 RNA seq datasets above 1000 RPMs (see **Supplementary Table 6**).

550 Sylamer analysis²⁹ was used to find enrichment of small word motifs in the 3'UTRs of genes enriched in
551 those that are most downregulated. A list of 3'UTRs was generated by eliminating repetitive regions as
552 described previously²⁰ to use for the Sylamer analysis. Default settings were used. Bonferroni adjusted p-
553 values were calculated by multiplying the unadjusted p-values by the number of permutations for each length
554 of word searched for.

555 The GO enrichment analyses shown in **Fig. 4f** and **Fig. S6b** were performed using the GOrilla GO
556 analysis tool at <http://cbl-gorilla.cs.technion.ac.il> using default setting using different p-value cut-offs for
557 each analysis. GO analysis in **Supplementary Table S5** was done using DAVID 6.8
558 (<https://david.ncifcrf.gov>) using default settings. GO analyses across multiple data sets were performed using
559 the software available on www.Metascape.org and default running parameters.

560 Density plots showing the contribution of the four nucleotides G, C, A and U at each of the 6mer seed
561 positions were generated using the Weblogo tool at <http://weblogo.berkeley.edu/logo.cgi> using the frequency
562 plot setting.

563 Venn diagrams were generated using <http://bioinformatics.psb.ugent.be/webtools/Venn/> using default
564 settings.

565 The scatter plot in **Fig. 4e** was generated using R package ggplot2. 10875 genes with RPM > 1 (average
566 RPM of the 8 RNAseq samples) and adjusted p-value < 0.05 were included. 3696 genes were significantly
567 upregulated in both mir-34a-5p and si34a-5p^{Seed} treated samples. 4207 genes were significantly
568 downregulated in both mir-34a-5p and si34a-5p^{Seed} treated samples. 713 genes were only downregulated and
569 792 genes were only upregulated in si34a-5p^{Seed} treated samples. 730 genes were only downregulated and
570 737 genes were only upregulated in mir-34a-5p treated samples. 193 genes out of the total 10875 genes were
571 omitted in the graph as the range for X and Y axes were set as -3 to 3.

572

573 **Identification the 6mer seeds most and least toxic to human cancer cells.**

574 To identify the 20 and 100 most and least toxic seeds to both human cell lines all 4096 seeds were ranked
575 for each cell line from highest to lowest toxicity. The 20 seeds with the highest toxicity to both HeyA8 and
576 H460 cells were found in the top 46 most toxic seeds to in both cells and the 20 seeds shared to be least toxic
577 were found in the bottom 149 seeds in each ranked group. The 100 most and least toxic seeds for both cell
578 lines were identified in the same way and all groups of seeds are shown in **Supplementary Table 2**.

579

580 **Metaplots of 6-mer seed match locations**

581 3pUTR sequences were downloaded from Ensembl Biomart. In order to reduce redundancy in the sequences,
582 a single longest 3pUTR (and associated transcript) was chosen to represent each gene. A custom perl script
583 (makeSeedBed.pl) was written to identify exact matches to all seeds (reverse complement) in all sequences,
584 and to output the coordinates of those matches in bed file format. A custom R script (plotBedMetaPlot.R)
585 was written that uses the GenomicRanges (<https://doi.org/10.1371/journal.pcbi.1003118>) and Sushi
586 (<https://dx.doi.org/10.1093%2Fbioinformatics%2Fbtu379>) R packages to calculate the coverage of seeds
587 across all sequences in a given set, and to create a plot of that coverage. The custom scripts and the input
588 data are available in the cloud-based computational reproducibility platform Code Ocean at
589 <https://codeocean.com/capsule/9a3eb292-6e89-44f0-b9b0-bdd779f97516/code>.

590

591 **eCDF plots**

592 A custom perl script (annotateWithSeeds.pl) was written to identify exact seed matches (reverse
593 complement) to all seeds in all sequences, and to output the total counts of the different types of seeds
594 (generally toxic vs. nontoxic) in the sequences. To compare the presence of toxic and nontoxic seed matches
595 in expression matched survival and non survival genes, a custom R script (makeECDFplot.180615.R) was
596 written that takes as input two different sets of genes (SGs and nonSGs) and the list of the counts of toxic
597 and nontoxic seeds (reverse complement) in all genes, and plots the cumulative distribution function for the
598 count statistics in each gene set. In **Fig. 3b** the ratio of the seed match counts to the 20 most and least toxic
599 seeds in the 5'UTR, CDS, first 1000bp of 3'UTR, and full 3'UTR (not shown) were compared between pairs
600 of 938 expression matched survival and non-survival genes. In **Fig. S5a**, this analysis was repeated with the
601 100 most and least toxic seeds to both human cell lines. The custom scripts and the input data are available in
602 the cloud-based computational reproducibility platform Code Ocean at
603 <https://codeocean.com/capsule/b755ec2b-00d8-4281-9fa1-2a484fd7521b/code>. To determine the dependence
604 of mRNAs regulation on miR-34a-5p seed presence in their 3'UTR, a custom R script
605 (makeECDFplot.cetoData.R) was written that takes as input a list of gene sets and a table of logFC
606 expression for those genes upon miR-34a-5p or si34a-5p^{Seed} over-expression. This Rscript then plots the
607 cumulative distribution function for the logFC expression data in each gene set. The custom scripts and the

608 input data are available in the Code Ocean at <https://codeocean.com/capsule/31ec8deb-8282-4a90-98e6->
609 [b80a0ba881cb/code](https://codeocean.com/capsule/31ec8deb-8282-4a90-98e6-b80a0ba881cb/code).

610

611 **Relation between miRNA seed conservation, age and toxicity**

612 Information on miRNA seed family conservation and seed sequence were downloaded at
613 http://www.targetscan.org/vert_71/ from TargetScan Human 7.1. The toxicity of each mature human miRNA
614 arm sequence in the TargetScan dataset was assigned according to the average toxicity induced by the
615 siRNA in HeyA8 and H460 siRNA screens harboring the identical 6mer seed sequence. A list of miRNA
616 ages corresponding to ~1025 miRNA loci was acquired from ³¹ and was calculated using a modified version
617 of ProteinHistorian ³¹. This list was used to assign ages to roughly ~1400 mature miRNA arms found in the
618 TargetScan dataset.

619 TargetScan 7.1 partitions the seed family conservation into four groups: highly conserved (group #2),
620 conserved (group #1), low conservation but still annotated as a miRNA (group #0), and low conservation
621 with the possibility of misannotation (group #-1). Probability density and eCDF plots for the assigned seed-
622 dependent toxicity were generated for each seed family conservation group using ggplot2 in R. Probability
623 density and eCDF plots were also generated to show how young (<10 million years) and old (>800 million
624 years) miRNAs compare in terms of the seed-dependent toxicity. All differences between groups in terms of
625 seed-dependent toxicity (always the average of the toxicity determined in HeyA8 and H460 cells) were
626 analyzed using a two-sample two-tailed Kolmogorov-Smirnov test in R.

627

628 **Assessment of dominant arm seed toxicity**

629 The expression (RPM) of miRNA 5p and 3p arms across 135 tissue samples were collected from MIRMINE
630 ⁵⁶. A miRNA was considered expressed if the sum of the normalized reads for both arms was above 5 for
631 each sample. A value of 0 was replaced with 0.01 to avoid a division by 0 error. A miRNA arm was
632 considered the dominant species if its expression was at least 25% greater than the other arm per sample. The
633 dominant arm for each miRNA across all samples was calculated by determining which arm was dominantly
634 expressed in more samples (>50% of samples where the miRNA was considered expressed). The miRNAs
635 that have only one annotated arm in miRBase were considered to have only one dominant arm. The seed
636 toxicity values for each arm were extracted from the 4096 siRNA screen data (% average viability for the
637 human HeyA8 and H460 cells) and used to calculate the ratio between the dominant arm's toxicity and the
638 lesser arm's toxicity; miRNAs that only had one expressed arm were not considered in the analyses shown in
639 **Fig. 5d** but are all included on the website: 6merdb.org.

640 To compare the 6mer seed toxicity between up regulated and down regulated Ago bound miRNA
641 populations in HCT116 cells after Doxo treatment we analyzed the reads obtained from RNA Seq analysis of

642 Ago bound RNAs. After removing the reads that were either shorter than 19 nt or longer than 26 nt in
643 length, the reads were blasted against a miRNA database consisting of all human miRNA mature sequence
644 information obtained from miRBase. A threshold of 100% identity for an at least 16 nt-long stretch without
645 any gaps was set for the BLAST analysis. After discarding sequences with no significant BLAST result, the
646 remaining sequences were trimmed from the 3' end so that all reads were now 19nt in length. This was done
647 to determine for each miRNA the relevant 5' end to obtain the 6mer seed sequence (position 2-7). All the
648 reads that shared the same 5' sequence and miRNA names were collapsed while adding up the number of
649 reads of each sequence in each condition. To compare the 6mer seed toxicity between up and down regulated
650 miRNAs, we calculated the average 6mer seed toxicity for miRNA sequences that were either 1.5 fold up or
651 1.5 fold down regulated in Doxo treated wt samples compared to medium treated control samples (after
652 removing sequences that had less than 100 collapsed reads in Doxo treated wt samples). In each group
653 miRNAs were ranked according to highest base mean expression and groups were compared. Statistically
654 significance was determined using the Mann-Whitney U test. The comparison was repeated for Drosha k.o.
655 cells where the 5' shifted form of miR-320a-3p was the only miRNA found to be upregulated (1.5 fold).

656

657 **Analysis of miRtron and non-miRtron groups**

658 MiRtrons and non-miRtrons were recently reported ⁵⁷ and consisted of miRNAs that are listed in miRBase
659 v21 as expressing both arms. Comparing 6mer toxicity of miRtrons and non-miRtrons from this list was
660 done as described above for young/old non-conserved/conserved miRNAs. Both arms were considered.
661 Probability density (**Fig. 5c**) and eCDF plots (**Fig. S7c**) were generated to show how miRtrons and non
662 miRtrons compare in terms of the seed-dependent toxicity.

663

664 **Comparing the seed viability of shRNAs derived from the CD95L sequence**

665 An RNAi lethality screen composed of every shRNA sequence that can be derived from the CD95L CDS
666 was conducted previously (20). In this screen, toxicity of each shRNA was assessed in two ways: 1) fold
667 underrepresentation of the shRNA after infection with the shRNA-expressing lentivirus compared to its
668 representation in the plasmid pool and 2) fold representation of the shRNA after infection and treatment with
669 doxycycline compared to cells that were infected but did not receive doxycycline. The first analysis allowed
670 us to quantify toxicity associated with "leaky" shRNA expression. The second analysis quantified toxicity
671 associated with strong shRNA expression following treatment with doxycycline.

672 For each shRNA, the average fold downregulation was calculated from both of these toxicity assessments.
673 Then, the seed sequence of each shRNA was extracted and assigned an average viability score, which was a
674 composite of the % viabilities determined in the 4096 siRNA arrayed screen for both HeyA8 and H460 cells.

675 Pearson's correlation was determined for each CD95L-derived shRNA between its associated fold
676 downregulation in the screen (20) and the average seed sequence viability determined in the 4096 siRNA
677 screen.

678 In addition, the CD95L shRNAs were split into two groups: 1) 137 shRNAs with an average fold
679 downregulation (as determined in the shRNA lethality screen) above 5 and 2) a control group with a
680 matching number of shRNAs whose fold deregulation had an absolute value closest to 0. The average seed
681 viability (as determined from the siRNA screen) was extracted for the shRNAs in these two groups and
682 compared using the two-sample, two-tailed Rank Sum test.

683

684 **Statistical analyses**

685 Continuous data were summarized as means and standard deviations (except for all IncuCyte experiments
686 where standard errors are shown) and dichotomous data as proportions. Continuous data were compared
687 using t-tests for two independent groups and one-way ANOVA for 3 or more groups. For evaluation of
688 continuous outcomes over time, two-way ANOVA was performed using the Stata 14 software with one
689 factor for the treatment conditions of primary interest and a second factor for time treated as a categorical
690 variable to allow for non-linearity. Comparisons of single proportions to hypothesized null values were
691 evaluated using binomial tests. Statistical tests of two independent proportions were used to compare
692 dichotomous observations across groups. Pearson correlation coefficients (r) and p - values as well as Mann
693 Whitney U test were calculated using StatPlus (v. 6.3.0.5). Kolmogorov–Smirnov two-sample two-sided test
694 was used to compare different probability distributions shown in all density plots and eCDF plots. Wilcoxon
695 rank sum test was used to test for statistical significance in the analysis of the toxicity all miRNA arms in

696 **Fig. 5d.**

697 The effects of treatment vs. control over time were compared for Drosha k.o. and wild-type cells by
698 fitting regression models that included linear and quadratic terms for value over time, main effects for
699 treatment and cell type, and two- and three-way interactions for treatment, cell-type and time. The three-way
700 interaction on the polynomial terms with treatment and cell type was evaluated for statistical significance
701 since this represents the difference in treatment effects over the course of the experiment for the varying cell
702 types.

703

704 **Data availability**

705 RNA sequencing data generated for this study is available in the GEO repository: GSE111379
706 (<https://www.ncbi.nlm.nih.gov/geo/query/acc.cgi?acc=GSE111379>, reviewer access token: srileykjtctduz)
707 and GSE111363 (<https://www.ncbi.nlm.nih.gov/geo/query/acc.cgi?acc=GSE111363>, reviewer access token:

708 udedukauvjexbmp). All 6mer seed toxicity data of the 4096 siRNA screen in HeyA8, H460, M565, and
709 3LL cells are available in searchable form at <https://6merdb.org>. All source data are available upon request.
710

711 **ACKNOWLEDGEMENTS**

712 We are indebted to Dr. Leon Platanius for his generous support of the seed screen and to Denise Scholtens
713 for help with biostatistics. M.H. was supported by the Intramural Research Program of NIAMS and A.A.S.
714 by the Swedish Research Council postdoctoral fellowship. This work was funded by training grant
715 T32CA009560 (to W.P.), R35CA197450 (to M.E.P.), R50CA221848 (to E.T.B.), and RO1 211916 (to EL).

716

717 **AUTHOR CONTRIBUTIONS**

718 M.E.P., Q.Q.G., W.E.P. and A.E.M. conceived the study. Q.Q.G., W.E.P. performed the majority of the
719 experiments and data analysis. S.C. performed the 6mer seed screens. A.A.S. performed the Ago pull-down
720 experiments. E.T.B. performed data analyses. J.M.P designed and implemented the website. M.H. provided
721 critical conceptual input. M.E.P. designed the study, guided the interpretation of the results and drafted the
722 manuscript. All authors discussed the results, edited and approved the draft and final versions of the
723 manuscript.

724

725 **DECLARATION OF INTEREST**

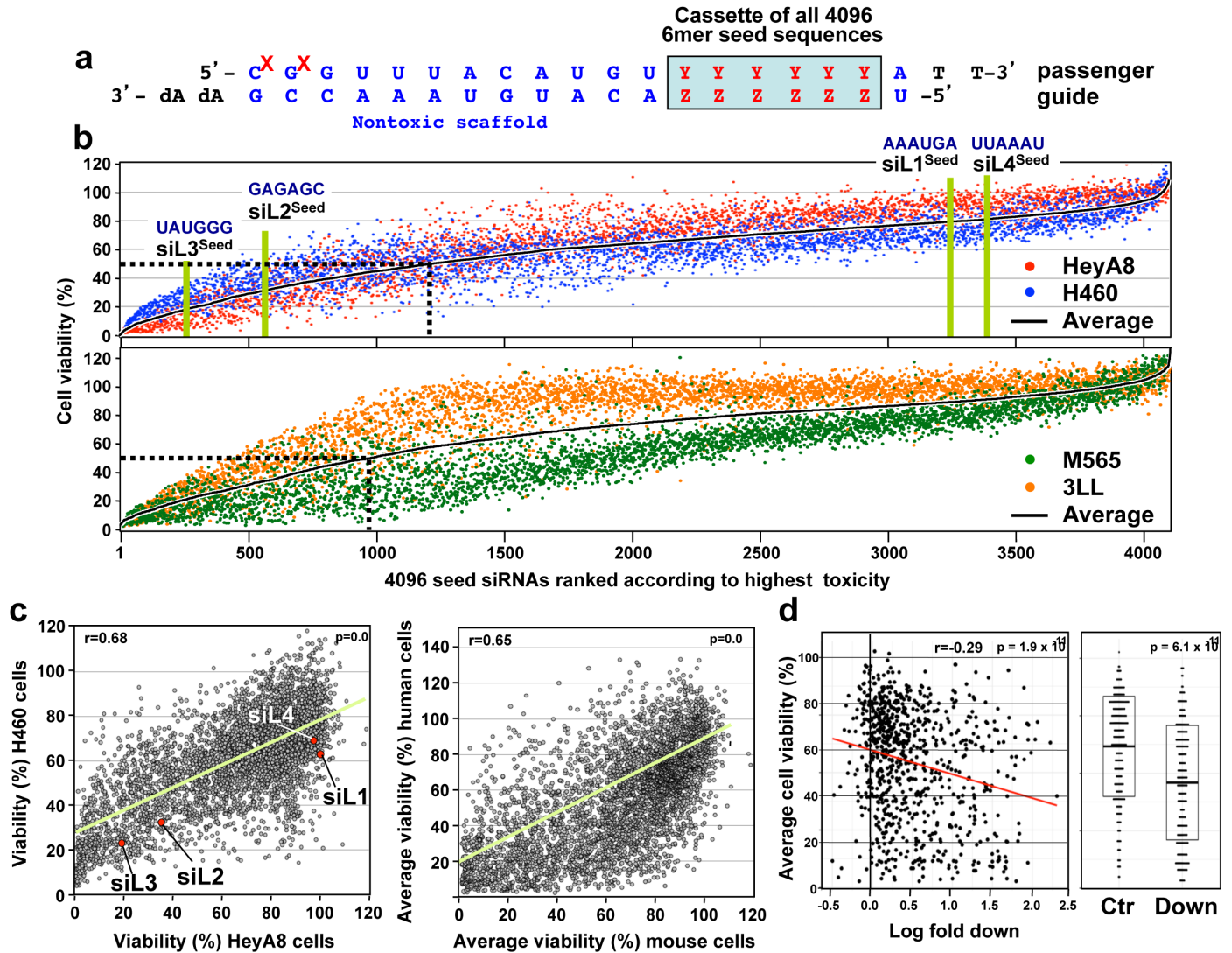
726 The authors declare no competing interests.

727

728

729

730 **Figures**



731

732

733

734

735

736

737

738

739

740

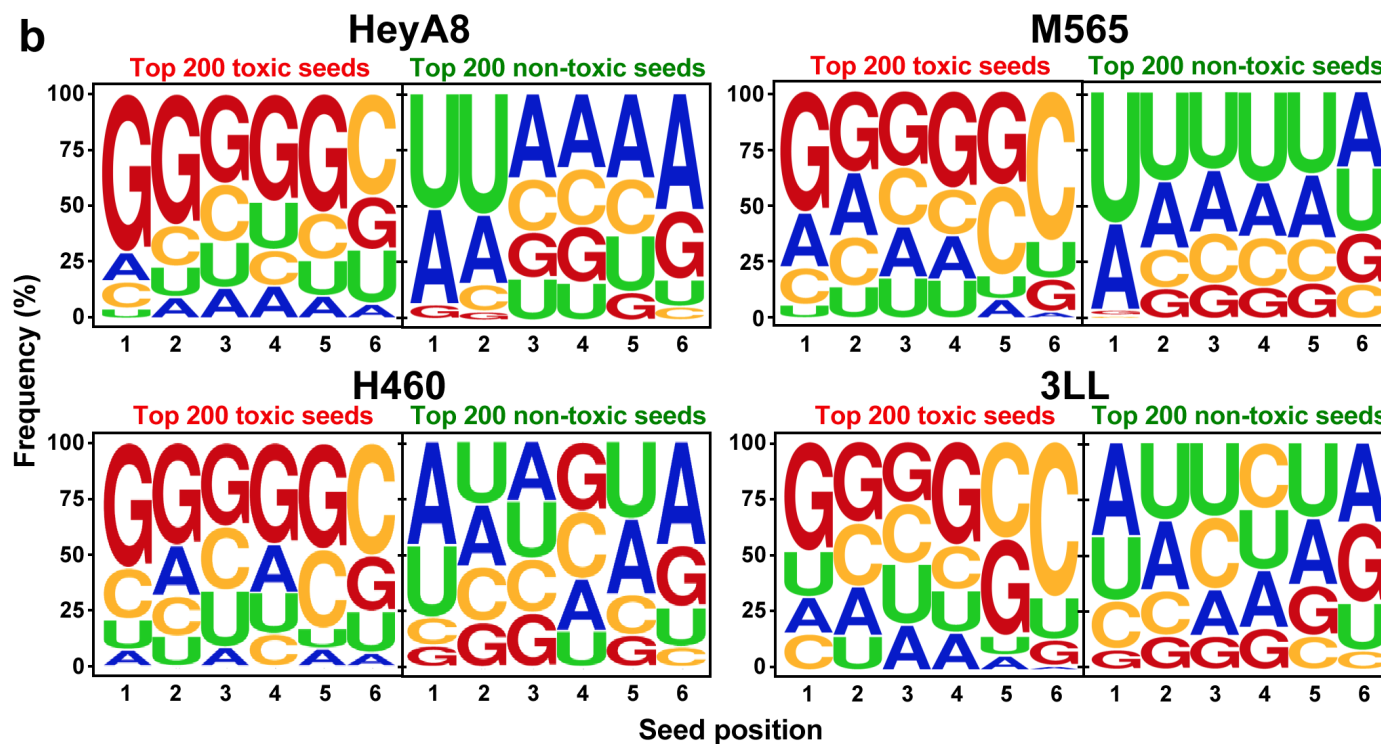
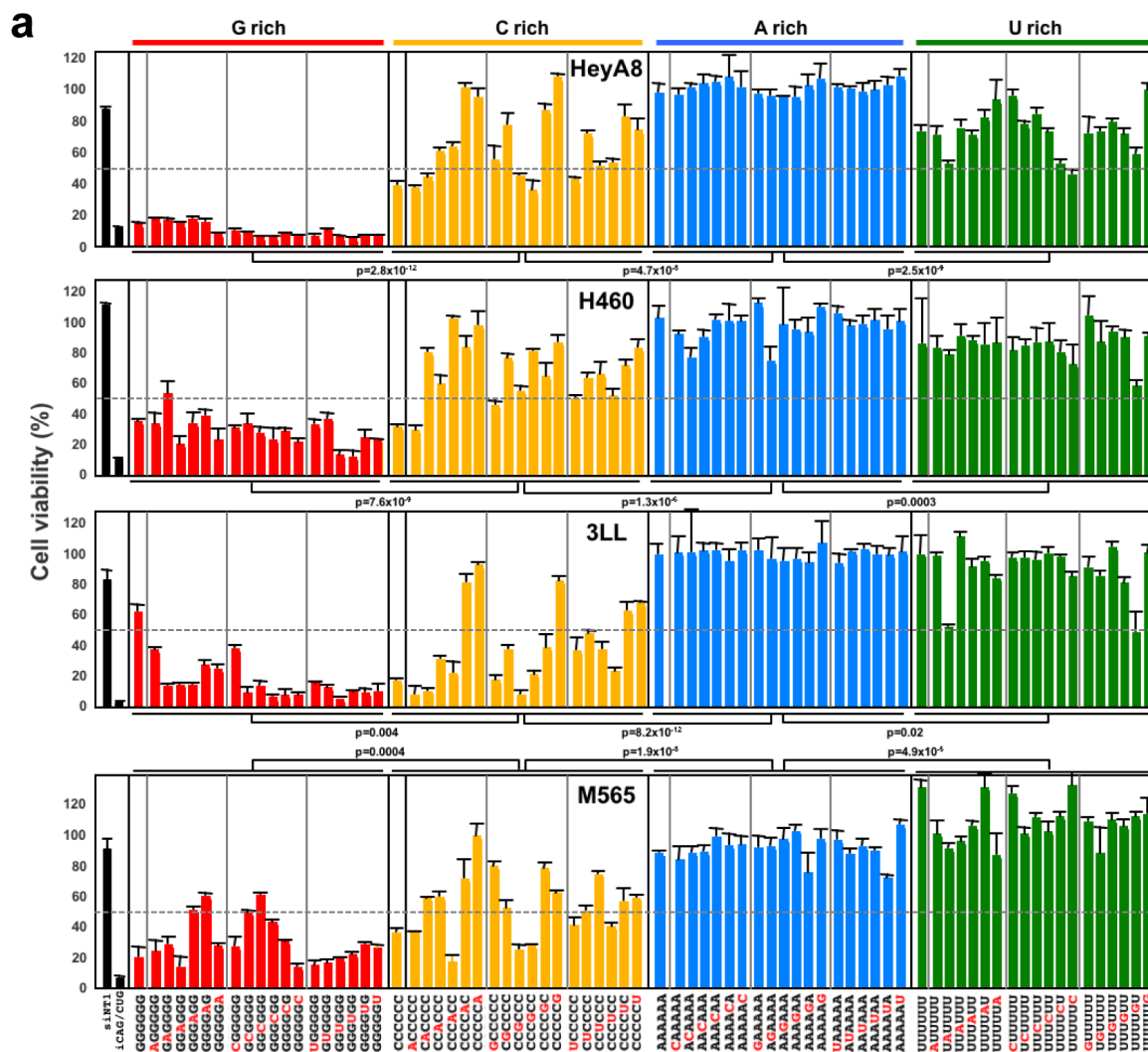
741

742

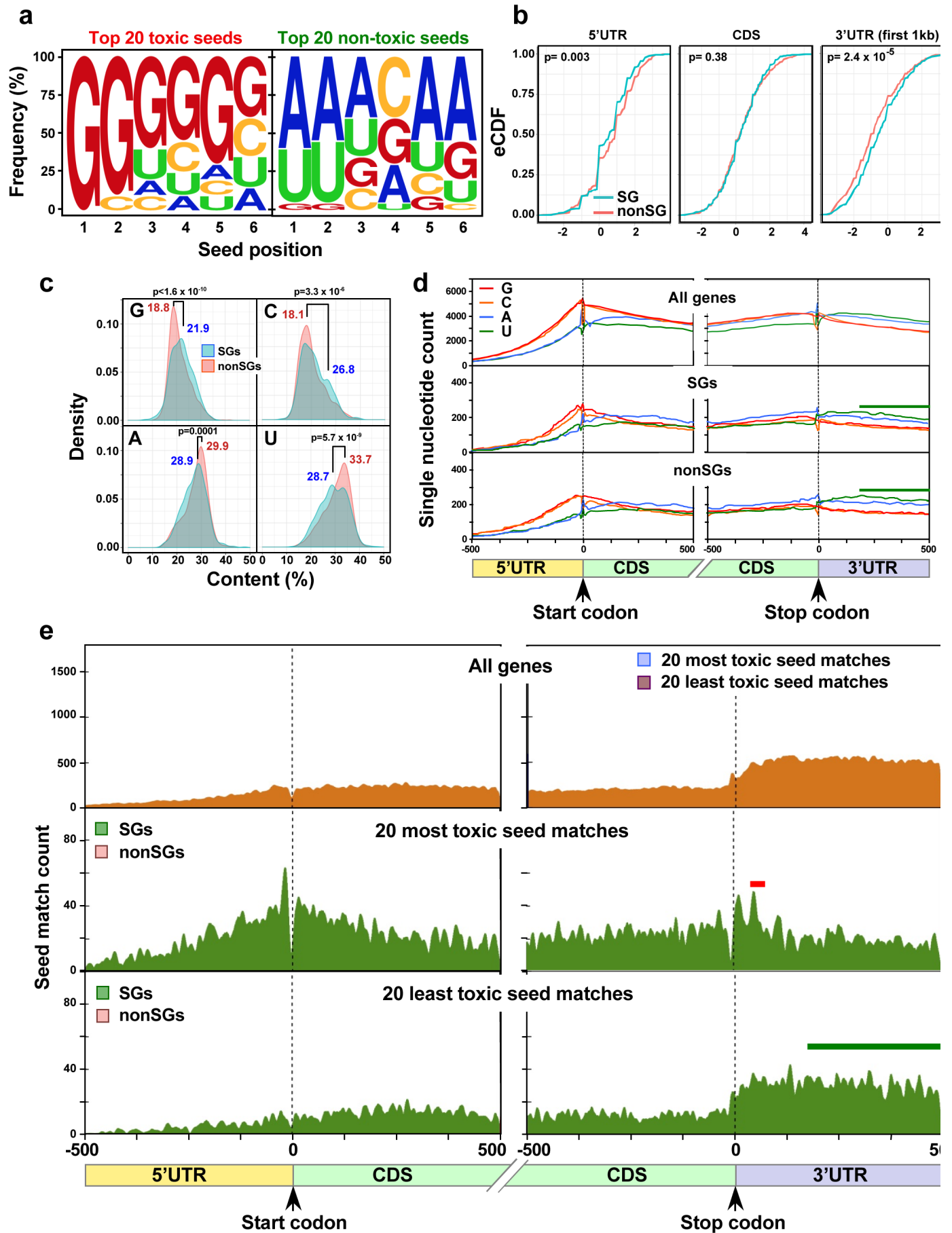
743

Fig. 1 A comprehensive screen identifies the most toxic 6mer seeds. **a** Schematic of the siRNA backbone used in the 4096 seed duplexes toxicity screen. 2'-O-methylation modifications at position 1 and 2 of the passenger strand were added to prevent passenger strand loading (marked by red Xs)²². The nucleotides that remained constant in all the duplexes are in blue. The variable 6mer seed sequence is in red (Y and complementary Z) and boxed in blue. **b** *Top*: Results of the 4096 6mer seed duplex screen in human HeyA8 and H460 cells. *Bottom*: Results of the 4096 6mer seed duplex screen in mouse M565 and 3LL cells. Cells were reverse transfected in triplicates in 384 well plates with 10 nM of individual siRNAs. The cell viability of each 6mer seed duplex was determined by quantifying cellular ATP content 96 hours after transfection. All 4096 6mer seeds are ranked by the average effect on cell viability of the two cell lines from the most toxic (left) to the least toxic (right). Rankings of the 6mer seeds of four previously characterized CD95L derived siRNAs (siL1, siL2, siL3, and siL4) are highlighted in green. We consider an siRNA highly toxic if it reduces cell viability 90% or more and moderately toxic if it reduces cell viability 50% or more (black

744 stippled line). **c** Regression analysis showing the correlation between the 6mer seed toxicity observed in
745 the human lung cancer cell line H460 (y axis) and the matching 6mer toxicity observed in the human ovarian
746 cancer cell line HeyA8 (x axis) (left) and average toxicity in the two human cell lines (y axis) and two mouse
747 cell lines (x axis) (right). p-values were calculated using Pearson correlation analysis. Toxicity of siRNAs
748 and miRNAs in all four cell lines can be interrogated at <https://6merdb.org>. **d** *Left*: Correlation between the
749 \log_{10} (fold down underrepresentation) of all possible shRNAs that can be derived from the mRNA sequence
750 of CD95L following their expression from a DOX-inducible lentiviral vector²⁰ and the toxicity of their seed
751 sequences as determined in a 4096 arrayed siRNA screen (average of both human cell lines) representing
752 every seed 6mer permutation²⁰. *Right*: Difference in average seed toxicity between the 137 CD95L-derived
753 shRNAs downregulated at least 5 fold (= toxic) in this screen compared to a size matched group of 137
754 shRNAs that were the least altered in their abundance in that screen. Pearson correlation coefficient is given
755 as well as p-value (left) and p-value in analysis on the right was calculated using unpaired two arm ttest.
756

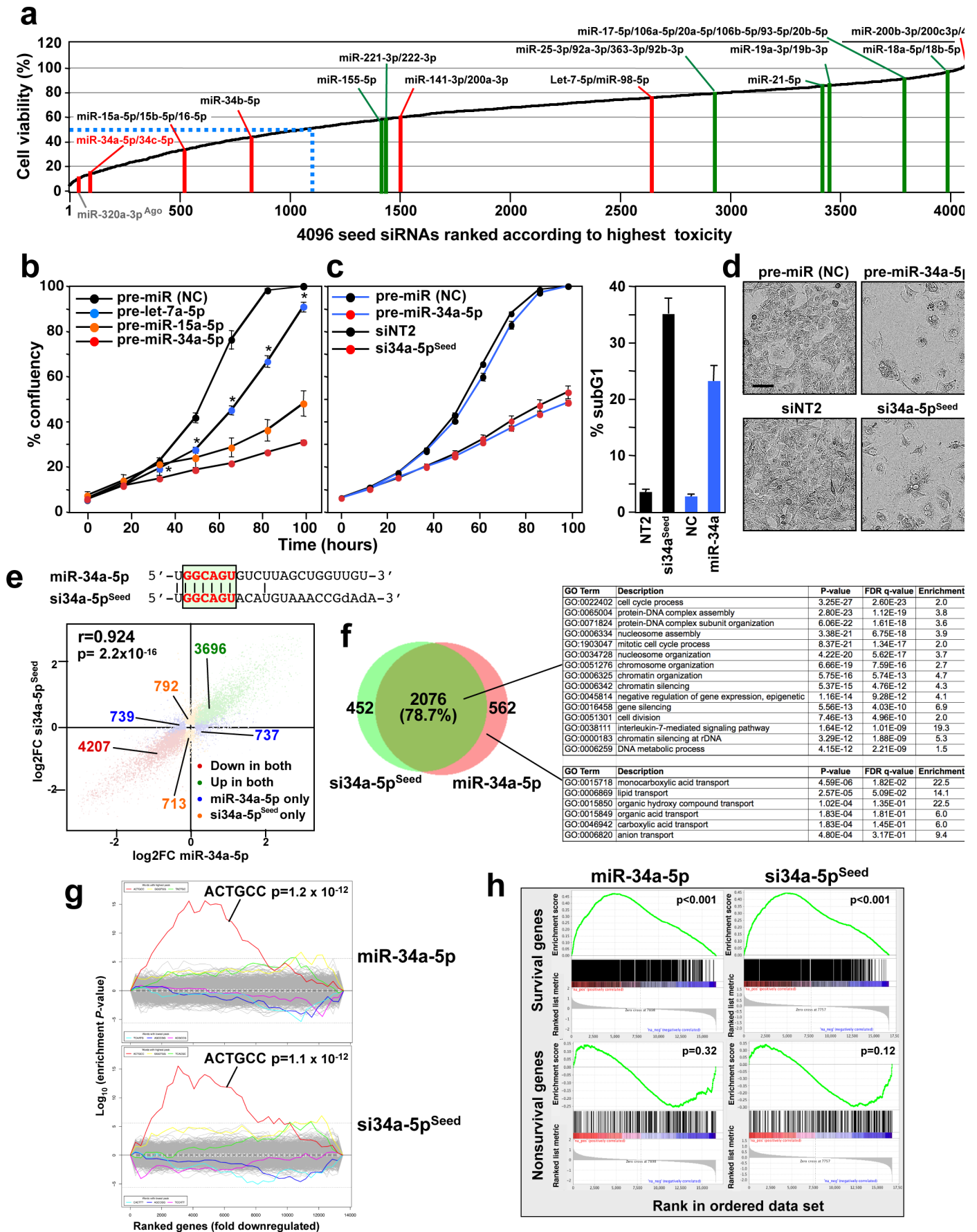


758 **Fig. 2** The most toxic seeds are G rich. **a** Cell viability of the 19 seed duplexes with the highest content
759 (>80%) in the 6mer seed region for each nucleotide in two human and two mouse cell lines. p-values
760 between groups of duplexes were calculated using Student's t-test. **b** Nucleotide composition at each of the 6
761 seed positions in the top 200 most toxic (left) or the top 200 least toxic (right) seed duplexes in the four cell
762 lines. siRNAs are considered to be toxic when viability is inhibited >50% (grey stippled line).
763



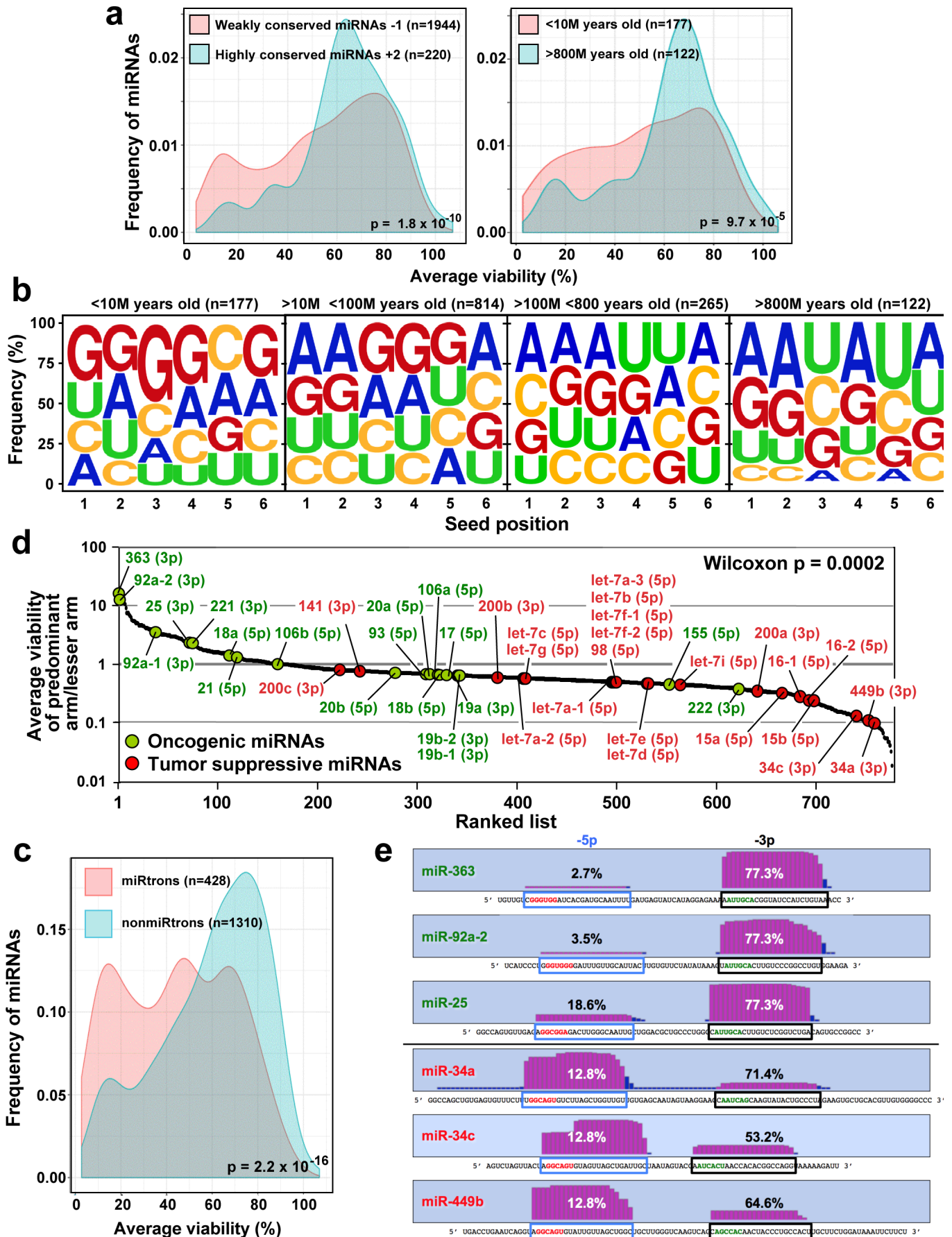
765 **Fig. 3** The most toxic G-rich seed containing duplexes preferentially target housekeeping genes enriched
766 in Cs close to the 3'UTR start site. **a** Nucleotide composition of 20 seeds that are most and least toxic in both
767 human cell lines (see **Fig. 1b**). **b** eCDF comparing the ratio of occurrences of the 20 most and least toxic
768 6mer seed matches in the mRNA elements of two sets of expression matched survival genes and nonsurvival
769 genes. Significance was calculated using a two-sample two-sided Kolmogorov–Smirnov (K-S) test.
770 Significance was higher in the analysis shown with the first 1000 bases of each 3'UTR than with the entire
771 3'UTR (data not shown). **c** Probability density plots comparing the nucleotide content between the groups of
772 expression matched SGs and nonSGs. p-values were calculated using a two-sample two-sided K-S test
773 comparing the density distribution of SGs and nonSGs. Relevant peak maxima are given. **d** Single nucleotide
774 frequency distribution in human mRNAs around the boundaries of the 5'UTR and the beginning of the CDS
775 and the end of the CDS and the beginning of the 3'UTR (shown are 500 bases in each direction). Data are
776 shown for either all human coding genes (top), a set of 938 SGs or an expression matched set of 938 nonSGs.
777 Green horizontal bars, area of reduced A/U content in SGs. **e** Distribution of the seed matches to the 20 most
778 and least toxic 6mer seeds to human cells in human mRNAs around the boundaries of the 5'UTR and the
779 beginning of the CDS and the end of the CDS and the beginning of the 3'UTR (shown are 500 bases in each
780 direction). Data are shown for either all genes (top) or the expression matched SGs and nonSGs (center and
781 bottom). Red horizontal bar, area of enriched toxic seed matches in SGs compared to nonSGs. Green
782 horizontal bar, area of fewer toxic seed matches in SGs.

783

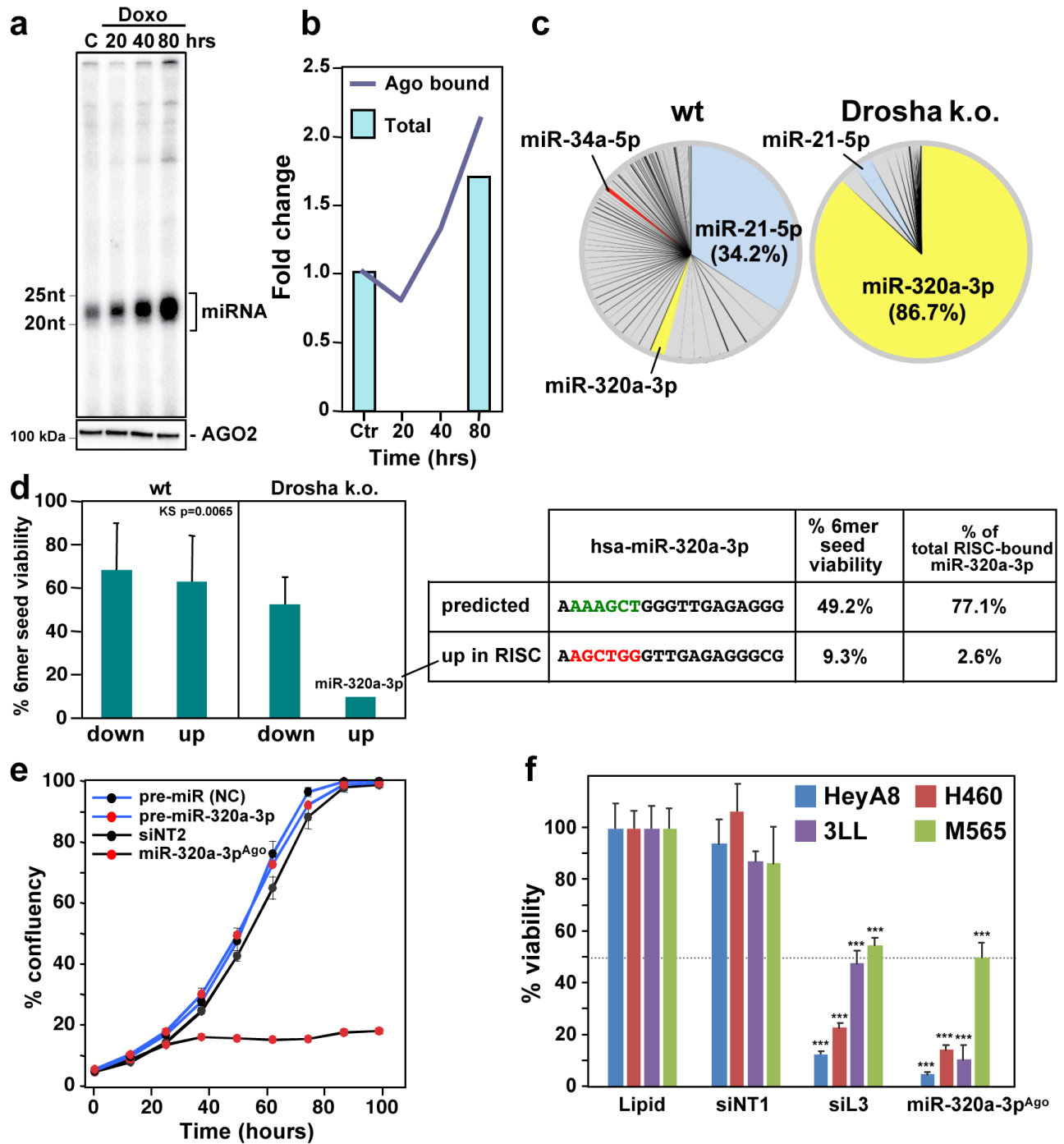


785 **Fig. 4** Tumor suppressive miRNAs inhibit cancer cell growth via toxic 6mer seeds. **a** All 4096 6mer
786 seeds ranked from the lowest average viability (highest toxicity) to the highest viability (lowest toxicity) in
787 HeyA8 and H460 cells. Locations of 6mer seeds present in major tumor suppressive (red) or tumor
788 promoting (green) miRNAs are highlighted as individual bars. miRNAs are considered to be toxic when
789 viability is inhibited >50% (blue stippled line). **b** Percent cell confluence over time of HeyA8 cells
790 transfected with 5 nM of either the indicated tumor suppressive miRNA precursors or a miRNA precursor
791 nontargeting control. Data are representative of two independent experiments. Each data point represents
792 mean \pm SE of four replicates. *Two-way ANOVA p-value between cells treated with pre-miR-(NC) and pre-
793 let-7a-5p is 0.0000. **c Left:** Percent cell confluence over time of HeyA8 parental cells transfected with either
794 pre-miR-34a-5p or si34a-5p^{Seed} and compared to their respective controls (pre-miR (NC) for pre-miR-34a
795 and siNT2 for si34a^{Seed}) at 10 nM. Data are representative of two independent experiments. Each data point
796 represents mean \pm SE of four replicates. **Right:** % cell death of the same cells harvested 4 days after
797 transfection. Data are representative of two experiments. Each data point represents mean \pm SD of three
798 replicates. **d** Morphology of HeyA8 cells transfected with either pre-miR-34a-5p or si34a-5p^{Seed} compared to
799 their respective controls at 10 nM three days after transfection. **e Top:** Alignment of the sequences of miR-
800 34a-5p and miR-34a-5p^{Seed} with the 6mer highlighted. **Bottom:** Comparison of deregulated mRNAs (adjusted
801 p<0.05, RPM > 1) in HeyA8 cells 48 hrs after transfection with either miR-34a-5p or si34a-5p^{Seed}. Pearson
802 correlation p-value is given. **f** Overlap of RNAs detected by RNA-Seq downregulated in HeyA8 cells (>1.5
803 fold) 48 hrs after transfection with either si34a-5p^{Seed} or miR-34a-5p when compared to either siNT2 or a
804 nontargeting pre-miR, respectively. **Right:** Results of a GOrilla gene ontology analyses of the genes
805 downregulated in both cells transfected with miR-34a-5p or si34a-5p^{Seed} (top, significance of enrichment <10⁻
806 ¹¹), or only in cells transfected with miR-34a-5p (bottom, significance of enrichment <10⁻⁴). **g** Sylamer plots
807 for the list of 3'UTRs of mRNAs in cells treated with either miR-34a-5p (top) or si34-5p^{Seed} (bottom) sorted
808 from down-regulated to up-regulated. The most highly enriched sequence is shown which, in each case, is
809 the 6mer seed match of the introduced 6mer seed. Bonferroni-adjusted p-values are shown. **h** Gene set
810 enrichment analysis for a group of 1846 survival genes (top 4 panels) and 416 non-survival genes (bottom 2
811 panels) ²⁰ after transfecting HeyA8 cells with either miR-34a-5p or si34a-5p^{Seed}. siNT1 and a nontargeting
812 premiR served as controls, respectively. p-values indicate the significance of enrichment.

813



815 **Fig. 5** Toxic 6mer seeds and the evolution of cancer regulating miRNAs. **a** Probability density plot of
816 cell viability of the 6mer seeds of either highly conserved (from humans to zebrafish) or poorly conserved
817 miRNA seed families (left panel, total number of mature miRNAs = 2164) or of very old (>800 Million
818 years) miRNAs or very young (<10 Million years) miRNAs (right panel, total number of miRNAs = 299).
819 For the analysis on the right, miRNA arms with identical sequences (gene duplications) were collapsed and
820 counted as one arm. Two-sample two-sided K-S test was used to calculate p-values. **b** Change in nucleotide
821 composition in the 6mer seeds of miRNAs of different ages. **c** Probability density plot of cell viability of the
822 6mer seeds of mature miRtrons or non-miRtrons. miRNAs with identical sequences (gene duplications) were
823 collapsed and counted as one seed. Two-sample two-sided K-S test was used to calculate p-value. **d** 780
824 miRNAs (**Supplementary Table 4**) ranked according to the ratio of viability of the seed (as determined in
825 the seed screen) of the guide strand and the lesser-expressed arm. Established oncogenic miRNAs are shown
826 in green, tumor-suppressive miRNAs are shown in red. The guide strand is given for each miRNA (in
827 parenthesis). p-value of the distribution of oncogenic versus tumor suppressive miRNAs was calculated
828 using two-sample two-sided K-S test. **e** Cumulative read numbers from the 5p or the 3p arm (according to
829 miRBase.org) of three oncogenic and three tumor-suppressive miRNAs with the highest (top three) or lowest
830 (bottom three) ratio of the viability of the guide strand versus the lesser arm. The viability numbers of the
831 matching 6mer seeds according to the siRNA 6mer seed screen are given. The sequences of the mature 5p or
832 3p arms are boxed in blue and black, respectively. Toxic seeds are shown in red, non-toxic ones in green.
833



834

835 **Fig. 6** Genotoxic drugs cause upregulation of tumor suppressive miRNAs. **a** *Top*: Plot of radiolabeled
 836 RNAs pulled down with the Ago proteins from HeyA8 cells treated with doxorubicin (Doxo) for 20, 40, or
 837 80 hours. *Bottom*: Western blot for the pulled down AGO2 of the same samples shown above. The images
 838 are representative of two biological duplicates. **b** Fold change of the total reads of Ago bound small RNAs
 839 after 20, 40, or 80 hours of Doxo treatment compared to the control sample from Ago-IP sequencing data
 840 (Ago bound). Fold change of the total reads of cytosolic small RNAs in HeyA8 cells treated with Doxo for
 841 80 hours compared to the control sample from small RNA-Seq data is given (Total). Data are the

842 combination of biological duplicates. **c** Pie charts showing the composition of miRNAs bound to Ago
843 proteins after 50 hrs Doxo treatment in HCT116 wild-type (left) or Drosha k.o. cells (right). **d** *Left*, 6mer
844 seed viability (average between HeyA8 and H460 cells) of the Ago-bound miRNAs most up and
845 downregulated in wt or Drosha k.o. cells after Doxo treatment. *Right*, Comparison of the predicted (and most
846 abundant) sequence of miR-320a-3p and Ago-bound sequence of miR-320a-3p and their average viability
847 found most upregulated in Drosha k.o. cells after Doxo treatment. Shown is variance of two biological
848 replicates. Mann-Whiney U test was used to calculate p-value. **e** Percent cell confluence over time of HeyA8
849 cells transfected with 5 nM of controls, pre-miR-320a or an siRNA duplex that corresponds to the shifted
850 form of miR-320a-3p (si-miR-320a-3p^{Ago}) that was found to be upregulated and bound to Ago proteins upon
851 Doxo treatment. Data are representative of two independent experiments. Each data point represents mean ±
852 SE of four replicates. **f** Viability changes (ATP content) in four cell lines 48 hrs after transfection with Lipid
853 only, 10 nM of siNT1, siL3, a nontargeting pre-miR, or miR-320a-3p^{Ago} - the only shared upregulated
854 miRNA in HeyA8 cells, HCT116 wild-type, and HCT116 Drosha k.o. cells - after Doxo treatment. p-values
855 were determined using Student's t-test. *** p<0.0001. Samples were performed in triplicate (siNT1, siL3), 6
856 repeats (miR-320a-3p^{Ago}) and 8 repeats (Lipid).

857

858 REFERENCES

859

- 860 1. Lee Y, *et al.* MicroRNA genes are transcribed by RNA polymerase II. *EMBO J* **23**, 4051-4060
861 (2004).
- 862 2. Han J, Lee Y, Yeom KH, Kim YK, Jin H, Kim VN. The Drosha-DGCR8 complex in primary
863 microRNA processing. *Genes Dev* **18**, 3016-3027 (2004).
- 864 3. Yi R, Qin Y, Macara IG, Cullen BR. Exportin-5 mediates the nuclear export of pre-microRNAs and
865 short hairpin RNAs. *Genes Dev* **17**, 3011-3016 (2003).
- 866 4. Bernstein E, Caudy AA, Hammond SM, Hannon GJ. Role for a bidentate ribonuclease in the
867 initiation step of RNA interference. *Nature* **409**, 363-366 (2001).
- 868 5. Hutvagner G, McLachlan J, Pasquinelli AE, Balint E, Tuschl T, Zamore PD. A cellular function for
869 the RNA-interference enzyme Dicer in the maturation of the let-7 small temporal RNA. *Science* **293**,
870 834-838 (2001).
- 871 6. Wang Y, Sheng G, Juranek S, Tuschl T, Patel DJ. Structure of the guide-strand-containing argonaute
872 silencing complex. *Nature* **456**, 209-213 (2008).
- 873 7. Leuschner PJ, Ameres SL, Kueng S, Martinez J. Cleavage of the siRNA passenger strand during
874 RISC assembly in human cells. *EMBO Rep* **7**, 314-320 (2006).
- 875 8. Schirle NT, MacRae IJ. The crystal structure of human Argonaute2. *Science* **336**, 1037-1040 (2012).
- 876 877 878 879 880 881 882 883

- 884 9. Eulalio A, Huntzinger E, Izaurralde E. GW182 interaction with Argonaute is essential for miRNA-
885 mediated translational repression and mRNA decay. *Nat Struct Mol Biol* **15**, 346-353 (2008).
886
- 887 10. Lewis BP, Shih IH, Jones-Rhoades MW, Bartel DP, Burge CB. Prediction of mammalian microRNA
888 targets. *Cell* **115**, 787-798 (2003).
889
- 890 11. Lai EC. Micro RNAs are complementary to 3' UTR sequence motifs that mediate negative post-
891 transcriptional regulation. *Nat Genet* **30**, 363-364 (2002).
892
- 893 12. Selbach M, Schwanhauss B, Thierfelder N, Fang Z, Khanin R, Rajewsky N. Widespread changes in
894 protein synthesis induced by microRNAs. *Nature* **455**, 58-63 (2008).
895
- 896 13. Baek D, Villen J, Shin C, Camargo FD, Gygi SP, Bartel DP. The impact of microRNAs on protein
897 output. *Nature* **455**, 64-71 (2008).
898
- 899 14. Esquela-Kerscher A, Slack FJ. Oncomirs - microRNAs with a role in cancer. *Nat Rev Cancer* **6**, 259-
900 269 (2006).
901
- 902 15. Balatti V, Pekarky Y, Rizzotto L, Croce CM. miR deregulation in CLL. *Adv Exp Med Biol* **792**, 309-
903 325 (2013).
904
- 905 16. Slabakova E, Culig Z, Remsik J, Soucek K. Alternative mechanisms of miR-34a regulation in cancer.
906 *Cell Death Dis* **8**, e3100 (2017).
907
- 908 17. Hua YJ, Larsen N, Kalyana-Sundaram S, Kjems J, Chinnaiyan AM, Peter ME. miRConnect 2.0:
909 Identification of antagonistic, oncogenic miRNA families in three human cancers. *BMC Genomics* **14**,
910 179 (2013).
911
- 912 18. Concepcion CP, Bonetti C, Ventura A. The microRNA-17-92 family of microRNA clusters in
913 development and disease. *Cancer journal* **18**, 262-267 (2012).
914
- 915 19. He X, He L, Hannon GJ. The guardian's little helper: microRNAs in the p53 tumor suppressor
916 network. *Cancer Res* **67**, 11099-11101 (2007).
917
- 918 20. Putzbach W, *et al.* Many si/shRNAs can kill cancer cells by targeting multiple survival genes through
919 an off-target mechanism. *eLife* **6**, e29702 (2017).
920
- 921 21. Murmann AE, *et al.* Induction of DISE in ovarian cancer cells in vivo. *Oncotarget* **8**, 84643-84658
922 (2017).
923
- 924 22. Murmann AE, *et al.* Small interfering RNAs based on huntingtin trinucleotide repeats are highly
925 toxic to cancer cells. *EMBO Rep* **19**, e45336 (2018).
926
- 927 23. Putzbach W, *et al.* CD95L mRNA is toxic to cells *bioRxive*, <https://doi.org/10.1101/330324> (2018).
928
- 929 24. Hadji A, *et al.* Death induced by CD95 or CD95 ligand elimination. *Cell Reports* **10**, 208-222 (2014).
930
- 931 25. Bramsen JB, *et al.* A large-scale chemical modification screen identifies design rules to generate
932 siRNAs with high activity, high stability and low toxicity. *Nucleic Acids Res* **37**, 2867-2881 (2009).
933

- 934 26. Peter ME. Let-7 and miR-200 microRNAs: guardians against pluripotency and cancer progression. *Cell Cycle* **8**, 843-852 (2009).
935
936
- 937 27. Agostini M, Knight RA. miR-34: from bench to bedside. *Oncotarget* **5**, 872-881 (2014).
938
- 939 28. Patel M, Peter ME. Identification of DISE-inducing shRNAs by monitoring cellular responses. *Cell Cycle* **17**, 506-514 (2018).
940
941
- 942 29. van Dongen S, Abreu-Goodger C, Enright AJ. Detecting microRNA binding and siRNA off-target effects from expression data. *Nat Methods* **5**, 1023-1025 (2008).
943
944
- 945 30. Grimson A, Farh KK, Johnston WK, Garrett-Engele P, Lim LP, Bartel DP. MicroRNA targeting specificity in mammals: determinants beyond seed pairing. *Mol Cell* **27**, 91-105 (2007).
946
947
- 948 31. Patel VD, Capra JA. Ancient human miRNAs are more likely to have broad functions and disease associations than young miRNAs. *BMC Genomics* **18**, 672 (2017).
949
950
- 951 32. Berezikov E, Chung WJ, Willis J, Cuppen E, Lai EC. Mammalian mirtron genes. *Mol Cell* **28**, 328-336 (2007).
952
953
- 954 33. Meijer HA, Smith EM, Bushell M. Regulation of miRNA strand selection: follow the leader? *Biochem Soc Trans* **42**, 1135-1140 (2014).
955
956
- 957 34. Concepcion CP, *et al.* Intact p53-dependent responses in miR-34-deficient mice. *PLoS Genet* **8**, e1002797 (2012).
958
959
- 960 35. Meredith AM, Dass CR. Increasing role of the cancer chemotherapeutic doxorubicin in cellular metabolism. *J Pharm Pharmacol* **68**, 729-741 (2016).
961
962
- 963 36. Yeung TK, Germond C, Chen X, Wang Z. The mode of action of taxol: apoptosis at low concentration and necrosis at high concentration. *Biochem Biophys Res Commun* **263**, 398-404 (1999).
964
965
966
- 967 37. Yoo SH, *et al.* Etoposide induces a mixed type of programmed cell death and overcomes the resistance conferred by Bcl-2 in Hep3B hepatoma cells. *Int J Oncol* **41**, 1443-1454 (2012).
968
969
- 970 38. Kwon HK, *et al.* Etoposide Induces Necrosis Through p53-Mediated Antiapoptosis in Human Kidney Proximal Tubule Cells. *Toxicol Sci* **148**, 204-219 (2015).
971
972
- 973 39. Wang D, Lippard SJ. Cellular processing of platinum anticancer drugs. *Nat Rev Drug Discov* **4**, 307-320 (2005).
974
975
- 976 40. Chang BD, *et al.* A senescence-like phenotype distinguishes tumor cells that undergo terminal proliferation arrest after exposure to anticancer agents. *Cancer Res* **59**, 3761-3767 (1999).
977
978
- 979 41. Eom YW, *et al.* Two distinct modes of cell death induced by doxorubicin: apoptosis and cell death through mitotic catastrophe accompanied by senescence-like phenotype. *Oncogene* **24**, 4765-4777 (2005).
980
981
982

- 983 42. Hauptmann J, *et al.* Biochemical isolation of Argonaute protein complexes by Ago-APP. *Proc*
984 *Natl Acad Sci U S A* **112**, 11841-11845 (2015).
985
- 986 43. Kim YK, Kim B, Kim VN. Re-evaluation of the roles of DROSHA, Exportin 5, and DICER in
987 microRNA biogenesis. *Proc Natl Acad Sci U S A* **113**, E1881-1889 (2016).
988
- 989 44. Walz AL, *et al.* Recurrent DGCR8, DROSHA, and SIX homeodomain mutations in favorable
990 histology Wilms tumors. *Cancer Cell* **27**, 286-297 (2015).
991
- 992 45. Kumar MS, Lu J, Mercer KL, Golub TR, Jacks T. Impaired microRNA processing enhances cellular
993 transformation and tumorigenesis. *Nat Genet* **39**, 673-677 (2007).
994
- 995 46. Chandradoss SD, Schirle NT, Szczepaniak M, MacRae IJ, Joo C. A Dynamic Search Process
996 Underlies MicroRNA Targeting. *Cell* **162**, 96-107 (2015).
997
- 998 47. Di Martino MT, *et al.* Synthetic miR-34a mimics as a novel therapeutic agent for multiple myeloma:
999 in vitro and in vivo evidence. *Clin Cancer Res* **18**, 6260-6270 (2012).
1000
- 1001 48. Beg MS, *et al.* Phase I study of MRX34, a liposomal miR-34a mimic, administered twice weekly in
1002 patients with advanced solid tumors. *Invest New Drugs* **35**, 180-188 (2017).
1003
- 1004 49. Cao W, *et al.* miR-34a regulates cisplatin-induced gastric cancer cell death by modulating
1005 PI3K/AKT/survivin pathway. *Tumour Biol* **35**, 1287-1295 (2014).
1006
- 1007 50. Navarro F, Lieberman J. miR-34 and p53: New Insights into a Complex Functional Relationship.
1008 *PLoS One* **10**, e0132767 (2015).
1009
- 1010 51. Alfano L, Costa C, Caporaso A, Antonini D, Giordano A, Pentimalli F. HUR protects NONO from
1011 degradation by mir320, which is induced by p53 upon UV irradiation. *Oncotarget* **7**, 78127-78139
1012 (2016).
1013
- 1014 52. Stark A, Brennecke J, Bushati N, Russell RB, Cohen SM. Animal MicroRNAs confer robustness to
1015 gene expression and have a significant impact on 3'UTR evolution. *Cell* **123**, 1133-1146 (2005).
1016
- 1017 53. Zare H, Khodursky A, Sartorelli V. An evolutionarily biased distribution of miRNA sites toward
1018 regulatory genes with high promoter-driven intrinsic transcriptional noise. *BMC Evol Biol* **14**, 74
1019 (2014).
1020
- 1021 54. Ceppi P, *et al.* CD95 and CD95L promote and protect cancer stem cells. *Nature Commun* **5**, 5238
1022 (2014).
1023
- 1024 55. Hafner M, Renwick N, Farazi TA, Mihailovic A, Pena JT, Tuschl T. Barcoded cDNA library
1025 preparation for small RNA profiling by next-generation sequencing. *Methods* **58**, 164-170 (2012).
1026
- 1027 56. Panwar B, Omenn GS, Guan Y. miRmine: a database of human miRNA expression profiles.
1028 *Bioinformatics* **33**, 1554-1560 (2017).
1029
- 1030 57. Rorbach G, Unold O, Konopka BM. Distinguishing mirtrons from canonical miRNAs with data
1031 exploration and machine learning methods. *Sci Rep* **8**, 7560 (2018).
1032

1033
1034